

The $T = 0$ random-field Ising model on a Bethe lattice with large coordination number: hysteresis and metastable states

M.L. Rosinberg

Laboratoire de Physique Théorique de la Matière Condensée, CNRS-UMR 7600, Université Pierre et Marie Curie, 4 place Jussieu, 75252 Paris Cedex 05, France

G. Tarjus

Laboratoire de Physique Théorique de la Matière Condensée, CNRS-UMR 7600, Université Pierre et Marie Curie, 4 place Jussieu, 75252 Paris Cedex 05, France

F.J. Pérez-Reche

Department of Chemistry, University of Cambridge, Cambridge, CB2 1EW, UK

Abstract.

In order to elucidate the relationship between rate-independent hysteresis and metastability in disordered systems driven by an external field, we study the Gaussian RFIM at $T = 0$ on regular random graphs (Bethe lattice) of finite connectivity z and compute to $O(1/z)$ (i.e. beyond mean-field) the quenched complexity associated with the one-spin-flip stable states with magnetization m as a function of the magnetic field H . When the saturation hysteresis loop is smooth in the thermodynamic limit, we find that it coincides with the envelope of the typical metastable states (the quenched complexity vanishes exactly along the loop and is strictly positive everywhere inside). On the other hand, the occurrence of a jump discontinuity in the loop (associated with an infinite avalanche) can be traced back to the existence of a gap in the magnetization of the metastable states for a range of applied field, and the envelope of the typical metastable states is then reentrant. These findings confirm and complete earlier analytical and numerical studies.

1. Introduction

At low temperature, disordered systems exhibit a large number of metastable states which are responsible for their slow relaxation dynamics and their irreversible, hysteretic response to an external field. In many cases this response is very well reproducible and independent of the rate at which the field is changed, provided it is low enough. This shows that these systems always explore the same set of metastable states when driven by the external field and that thermally activated processes are irrelevant on experimental time scales. Classical examples of such behavior are magnetic materials. When the external magnetic field is slowly cycled from large negative to large positive values and back, the induced magnetization displays a (saturation) hysteresis loop with a characteristic shape that depends on the mechanisms for the formation and evolution of the magnetic domains[1]. Other field histories give rise to a complicated subloop structure that is also well reproducible.

By definition, the future evolution of a hysteretic system depends on its past history, and the theory of rate-independent hysteresis generally focuses on a dynamical description in order to describe history-dependent effects such as return-point memory[1, 2, 3]. However, the hysteresis loop may also be viewed as a special path among the metastable states and one may wonder whether it is possible to characterize this path without having to follow the dynamical evolution. Surprisingly, a general answer to this question is not yet available. In the case of attractive (ferromagnetic) interactions, however, an important fact is known: if the dynamics obeys the so-called no-passing rule[2] (i.e. preserves some natural partial ordering of the microscopic configurations), there are no metastable states outside the saturation hysteresis loop[4]. Since, as a general rule, the number of metastable states scales exponentially with the system size, this result implies that the corresponding entropy density (or complexity) is not positive outside the loop. What still remains to be understood is the situation *inside* the loop.

A convenient framework for studying this problem is the zero-temperature Random Field Ising model (RFIM) driven by an external field. This is a model for disordered ferromagnets which is relevant to a large class of materials where disorder induces random fields[5]. With the standard Glauber dynamics (which does satisfy the no-passing rule at $T = 0$ [2]), the metastable states are the so-called single-spin-flip stable states, each state being characterized by its energy and magnetization. The quantity to be studied in relation to hysteresis is $\mathcal{N}(m, H)$, the number of metastable states at the field H with given magnetization per spin m . One can then reformulate the above question as follows: in which region of the field-magnetization plane is the logarithm of $\mathcal{N}(m, H)$ an extensive quantity? In particular, does the saturation hysteresis loop identifies with the boundary of this region? To answer these questions, one must study the properties of a *typical* system and compute the *quenched* complexity $\Sigma_Q(m, H)$ of the metastable states[4]. This is a nontrivial analytical or numerical task in general, and there exists very few results on the typical number of metastable states in finite-connectivity disordered spin systems. For the Gaussian RFIM, the only analytical

result so far has been obtained in one dimension[4] (or, equivalently, on a Bethe lattice of connectivity $z = 2$), showing that the curve $\Sigma_Q(m, H) = 0$ coincides with the hysteresis loop. Numerical results on the Bethe lattice of coordination $z = 4$ and on the cubic lattice[6] strongly suggest that this property always holds when the hysteresis loop is smooth in the thermodynamic limit (which occurs when the disorder is large enough). This means that the typical number of metastable states is exponentially large everywhere inside the loop[7]. The situation is more complicated when the loop has a jump at some critical value of the field, which corresponds to an out-of-equilibrium phase transition associated with the appearance of a macroscopic “avalanche”[2]. This happens at low disorder in three and higher dimensions[2, 8] or on a Bethe lattice for $z \geq 4$ [9] (the situation for $d = 2$ is still not settled[10]). It has been suggested[4] that this jump reveals the existence of a gap in the magnetization of the typical metastable states in a *finite* range of H , gap which may also explain the reentrant hysteresis loops observed when changing the driving mechanism[11]. This assumption is also supported by numerical computations[6], but again there is no analytical proof. The aim of the present work is to give further evidence to this scenario (both above and below the critical disorder) by computing analytically the quenched complexity of the Gaussian RFIM on a Bethe lattice to order $1/z$, and comparing with the exact expression of the hysteresis loop[9] at the same order. This will also help us to clarify the approach to the mean-field fully-connected limit[12].

The paper is organized as follows. In section II, we define the model and present the general formalism for calculating the quenched complexity. Section III is devoted to the mean-field limit which is recovered when $z \rightarrow \infty$. The calculation of the complexity at the order $1/z$ is presented in section IV and the numerical results are discussed in section V. We finish with a brief discussion and some perspectives in section VI. More details on the analytical calculations are given in the appendices.

2. General formalism

We start with the RFIM Hamiltonian

$$\mathcal{H} = -J \sum_{\langle i, j \rangle} s_i s_j - \sum_i (h_i + H) s_i \quad (1)$$

describing a collection of N Ising spins ($s_i = \pm 1$) placed on the vertices of a graph of connectivity z and submitted to an external uniform field H . A ferromagnetic interaction $J > 0$ couples the spin i to its z neighbours j and $\{h_i\}$ is a collection of random fields drawn identically and independently from a Gaussian probability distribution $\mathcal{P}(h)$ with zero mean and standard deviation Δ . In the zero-temperature system with metastable dynamics[2], the field H is adiabatically varied (for instance from $-\infty$ to $+\infty$ and back) and each spin is aligned with its local effective field

$$f_i = J \sum_{j/i} s_j + h_i + H \quad (2)$$

so that

$$s_i = \text{sgn}(f_i) . \quad (3)$$

In the thermodynamic limit, the resulting hysteresis loop $m(H)$ (where $m = (1/N) \sum_i s_i$ is the magnetization per spin) is smooth for $\Delta > \Delta_c(z)$ and discontinuous for $\Delta < \Delta_c(z)$, where $\Delta_c(z)$ is a critical value of the disorder at which avalanches of all sizes occur (an avalanche corresponds to a jump in the magnetization curve $m(H)$). A complete analytical description of this behavior is available in the mean-field model[2, 8] which can be obtained for instance by placing the spins on a fully-connected lattice. In this limit, there is no hysteresis above $\Delta_c^0 = \lim_{z \rightarrow \infty} \Delta_c(z) = J\sqrt{2/\pi}$ and the number of metastable states is not exponentially large[12] (but it may be larger than 1, even along the so-called “unstable” branch for $\Delta < \Delta_c^0$).

Our goal in this paper is to compute the first non-zero term in the $1/z$ expansion of the complexity $\Sigma_Q(m, H)$. Although the corrections to the mean-field result are certainly different on the Bethe lattice and on the hypercubic lattice, we only consider the former case since an analytical expression of the hysteresis curve is available for any z [9]. This also allows us to use the machinery developed in Ref.[4] to compute $\Sigma_Q(m, H)$. The possible influence of geometry will be briefly discussed in the conclusion.

$\Sigma_Q(m, H)$ is defined as

$$\Sigma_Q(m, H) = \lim_{N \rightarrow \infty} \frac{1}{N} \overline{\ln \mathcal{N}(m, H)} = \lim_{n \rightarrow 0} \frac{1}{n} \lim_{N \rightarrow \infty} \frac{1}{N} \left[\overline{\mathcal{N}(m, H)^n} - 1 \right] \quad (4)$$

where, as usual, the order of the limits $N \rightarrow \infty$ and the number of replicas $n \rightarrow 0$ has been inverted. The starting point of our calculation is the following expression of $\overline{\mathcal{N}(m, H)^n}$ in the large- N limit[4]:

$$\overline{\mathcal{N}(m, H)^n} \sim \int \prod_{a=1}^n dg^a \prod_{\boldsymbol{\sigma}, \boldsymbol{\tau}} dc(\boldsymbol{\sigma}, \boldsymbol{\tau}) e^{N\mathcal{F}(\{c\}, \mathbf{g})} \quad (5)$$

where

$$\mathcal{F}(\{c\}, \mathbf{g}) = \Lambda(\{c\}, \mathbf{g}) + \frac{z}{2} - \frac{z}{2} \sum_{\boldsymbol{\sigma}, \boldsymbol{\tau}} c(\boldsymbol{\sigma}, \boldsymbol{\tau}) c(\boldsymbol{\tau}, \boldsymbol{\sigma}) - m \sum_{a=1}^n g^a \quad (6)$$

and

$$\Lambda(\{c\}, \mathbf{g}) = \ln \sum_{\boldsymbol{\sigma}} \int \mathcal{P}(h) dh \int dx dy e^{iy \cdot (\mathbf{x} - \mathbf{H} - \mathbf{h})} \left[\sum_{\boldsymbol{\tau}} c(\boldsymbol{\tau}, \boldsymbol{\sigma}) e^{-iJy \cdot \boldsymbol{\tau}} \right]^z \prod_{a=1}^n e^{g^a \sigma^a} \Theta(x^a \sigma^a) \quad (7)$$

where $\Theta(x)$ is the Heaviside function. In these equations, the bold symbols denote n -component vectors in replica space, e.g. $\mathbf{x} = \{x^a; a = 1, \dots, n\}$, (with $\mathbf{h} = h\mathbf{1}$ and $\mathbf{H} = H\mathbf{1}$); $c(\boldsymbol{\sigma}, \boldsymbol{\tau})$ is an order parameter, function of the two binary vectors $\boldsymbol{\sigma}$ and $\boldsymbol{\tau}$ ($\sigma^a = \pm 1$, $\tau^a = \pm 1$), which allows the decoupling of the sums over the sites i . It generalizes the single-argument order-parameter function $c(\boldsymbol{\sigma})$ introduced in Ref. [13] to study finite-connectivity spin glasses (see also Ref.[14]). $\mathbf{g} = \{g^a\}$ is a set of Lagrange multipliers associated with the constraint $\sum_i s_i^a = Nm$ in each replica. (The interested

reader is referred to Ref. [4] for the derivation of these equations[15]. Apart from these three equations, the present paper is self-contained.)

In the large- N limit, the integral in Eq. (5) can be evaluated by the method of steepest descent. The 2^{2n} order parameters $c(\boldsymbol{\sigma}, \boldsymbol{\tau})$ and the n Lagrange multipliers g^a are determined through the saddle-point equations that correspond to the extremization of the functional $F(\{c\}, \mathbf{g})$,

$$c(\boldsymbol{\sigma}, \boldsymbol{\tau}) = \frac{1}{z} \frac{\partial \Lambda(\{c\}, \mathbf{g})}{\partial c(\boldsymbol{\tau}, \boldsymbol{\sigma})} \quad (8)$$

$$m = \frac{\partial \Lambda(\{c\}, \mathbf{g})}{\partial g^a}, \quad (9)$$

where a is any of the replicas $1, \dots, n$. One can easily see that the solution of Eq. (8) (that will be denoted as $c^*(\boldsymbol{\sigma}, \boldsymbol{\tau})$, dropping the dependence on \mathbf{g} and H) satisfies the normalization condition

$$\sum_{\boldsymbol{\sigma}, \boldsymbol{\tau}} c^*(\boldsymbol{\sigma}, \boldsymbol{\tau}) c^*(\boldsymbol{\tau}, \boldsymbol{\sigma}) = 1 \quad (10)$$

so that Eqs. (9) can be rewritten as[4]

$$m = \sum_{\boldsymbol{\sigma}, \boldsymbol{\tau}} \sigma^a c^*(\boldsymbol{\sigma}, \boldsymbol{\tau}) c^*(\boldsymbol{\tau}, \boldsymbol{\sigma}). \quad (11)$$

Assuming that the solution of Eq. (11) in the limit $n \rightarrow 0$ is the same for all replicas, namely $g^{*a} = g^*(m, H)$, we expand $\Lambda^*(m, H) \equiv \Lambda(c^*(\boldsymbol{\sigma}, \boldsymbol{\tau}), g^*)$ in powers of n ,

$$\Lambda^*(m, H) = \Lambda^{*(0)}(m, H) + n\Lambda^{*(1)}(m, H) + O(n^2), \quad (12)$$

which, after insertion in Eq.(5), yields

$$\Sigma_Q(m, H) = \Lambda^{*(1)}(m, H) - mg^*(m, H), \quad (13)$$

where we have used that $\Lambda^{*(0)}(m, H)$ is equal to zero, which is necessary to obtain a well-defined $n \rightarrow 0$ limit.

As discussed in Refs. [4, 6], it is in fact convenient to treat the Lagrange multiplier g as a free parameter and to consider that the magnetization is a function of g given by the solution of Eq. (11) in the limit $n \rightarrow 0$. Defining $\Lambda^*(g, H) \equiv \Lambda(c^*(\boldsymbol{\sigma}, \boldsymbol{\tau}), g)$, we then write

$$\Sigma_Q(g, H) \equiv \Sigma_Q(m^*(g, H), H) = \Lambda^{*(1)}(g, H) - m^*(g, H)g \quad (14)$$

where $m^*(g, H) = \lim_{n \rightarrow 0} \sum_{\boldsymbol{\sigma}, \boldsymbol{\tau}} \sigma^a c^*(\boldsymbol{\sigma}, \boldsymbol{\tau}) c^*(\boldsymbol{\tau}, \boldsymbol{\sigma}) = \partial \Lambda^{*(1)}(g, H) / \partial g$. In other words, $\Sigma_Q(m, H)$ and $\Lambda^{*(1)}(g, H)$ are mutually connected by a Legendre transform with $-g^*(m, H)$ being the slope of the complexity curve, i.e. $g^*(m, H) = -\partial \Sigma_Q(m, H) / \partial m$. It is crucial that the mapping $\{m^*(g, H), \Sigma_Q(g, H)\} \mapsto \Sigma_Q(m, H)$ is unambiguously defined, as will be discussed in section V. Note also that the total complexity at the field H , irrespective of the magnetization, is obtained by setting $g = 0$ in Eq.(14). This corresponds to the maximum of $\Sigma_Q(m, H)$ that occurs at a magnetization $m^{max}(H) = m^*(g = 0, H)$.

We now turn to the $1/z$ expansion of $\Sigma_Q(m, H)$. Using the rescaling $Jz \rightarrow J$, we rewrite Eq. (7) as

$$\Lambda(\{c\}, \mathbf{g}) = \ln \sum_{\boldsymbol{\sigma}} e^{g^s} \int \mathcal{P}(h) dh \int d\mathbf{x} d\mathbf{y} e^{\phi(\mathbf{x}, \mathbf{y})} \prod_a \Theta(x^a \sigma^a) \quad (15)$$

where $s = \sum_a \sigma^a$ and

$$\phi(\mathbf{x}, \mathbf{y}) = i\mathbf{y} \cdot (\mathbf{x} - \mathbf{H} - \mathbf{h}) + z \ln \sum_{\boldsymbol{\tau}} c(\boldsymbol{\tau}, \boldsymbol{\sigma}) e^{-i\frac{J}{z}\mathbf{y} \cdot \boldsymbol{\tau}}. \quad (16)$$

We then formally expand Eqs. (8) and (10) in powers of $1/z$, assuming that

$$\Lambda^*(g, H) = z\Lambda_{-1}^*(g, H) + \Lambda_0^*(g, H) + \frac{1}{z}\Lambda_1^*(g, H) + \dots \quad (17)$$

$$m^*(g, H) = m_0^*(g, H) + \frac{1}{z}m_1^*(g, H) + \dots \quad (18)$$

and

$$c^*(\boldsymbol{\sigma}, \boldsymbol{\tau}) = c_0^*(\boldsymbol{\sigma}, \boldsymbol{\tau}) + \frac{1}{z}c_1^*(\boldsymbol{\sigma}, \boldsymbol{\tau}) + \frac{1}{z^2}c_2^*(\boldsymbol{\sigma}, \boldsymbol{\tau}) + \dots \quad (19)$$

This yields a set of coupled equations to be solved at each order in $1/z$. The main difficulty of the calculation is that successive orders are not independent. Indeed, one has

$$\phi(\mathbf{x}, \mathbf{y}) = z \ln \left(\sum_{\boldsymbol{\tau}} c_0^*(\boldsymbol{\tau}, \boldsymbol{\sigma}) \right) + \phi_0(\mathbf{x}, \mathbf{y}) + \frac{1}{z}\phi_1(\mathbf{x}, \mathbf{y}) + \frac{1}{z^2}\phi_2(\mathbf{x}, \mathbf{y}) + \dots \quad (20)$$

with

$$\phi_0(\mathbf{x}, \mathbf{y}) = i\mathbf{y} \cdot (\mathbf{x} - \mathbf{H} - \mathbf{h}) + \frac{\sum_{\boldsymbol{\tau}} [c_1^*(\boldsymbol{\tau}, \boldsymbol{\sigma}) - iJ\mathbf{y} \cdot \boldsymbol{\tau} c_0^*(\boldsymbol{\tau}, \boldsymbol{\sigma})]}{\sum_{\boldsymbol{\tau}} c_0^*(\boldsymbol{\tau}, \boldsymbol{\sigma})} \quad (21a)$$

$$\phi_1(\mathbf{x}, \mathbf{y}) = \frac{\sum_{\boldsymbol{\tau}} [c_2^*(\boldsymbol{\tau}, \boldsymbol{\sigma}) - iJ\mathbf{y} \cdot \boldsymbol{\tau} c_1^*(\boldsymbol{\tau}, \boldsymbol{\sigma}) - \frac{J^2}{2}(\mathbf{y} \cdot \boldsymbol{\tau})^2 c_0^*(\boldsymbol{\tau}, \boldsymbol{\sigma})]}{\sum_{\boldsymbol{\tau}} c_0^*(\boldsymbol{\tau}, \boldsymbol{\sigma})} - \frac{1}{2} \left[\frac{\sum_{\boldsymbol{\tau}} [c_1^*(\boldsymbol{\tau}, \boldsymbol{\sigma}) - iJ\mathbf{y} \cdot \boldsymbol{\tau} c_0^*(\boldsymbol{\tau}, \boldsymbol{\sigma})]}{\sum_{\boldsymbol{\tau}} c_0^*(\boldsymbol{\tau}, \boldsymbol{\sigma})} \right]^2 \quad (21b)$$

etc.... Inserting Eq. (15) in Eq. (8) and using these expansions, we obtain

$$\Lambda_{-1}^* + \ln \sum_{\boldsymbol{\tau}} c_0^*(\boldsymbol{\tau}, \boldsymbol{\sigma}) = 0 \quad (22)$$

at leading order, and

$$c_0^*(\boldsymbol{\sigma}, \boldsymbol{\tau}) = e^{-\Lambda_0^* + g^s} \int \mathcal{P}(h) dh \int d\mathbf{x} d\mathbf{y} e^{\phi_0(\mathbf{x}, \mathbf{y})} \prod_a \Theta(x^a \sigma^a), \quad (23)$$

$$\begin{aligned} c_1^*(\boldsymbol{\sigma}, \boldsymbol{\tau}) = & e^{-\Lambda_0^* + g^s} \int \mathcal{P}(h) dh \int d\mathbf{x} d\mathbf{y} e^{\phi_0(\mathbf{x}, \mathbf{y})} \prod_a \Theta(x^a \sigma^a) \left[-\Lambda_1^* + \phi_1(\mathbf{x}, \mathbf{y}) - iJ\mathbf{y} \cdot \boldsymbol{\tau} \right. \\ & \left. - \sum_{\boldsymbol{\tau}'} [c_1^*(\boldsymbol{\tau}', \boldsymbol{\sigma}) - iJ\mathbf{y} \cdot \boldsymbol{\tau}' c_0^*(\boldsymbol{\tau}', \boldsymbol{\sigma})] \right] \end{aligned} \quad (24)$$

at the two next orders. Similarly, the expansion of the normalization equation, Eq. (10), yields

$$\sum_{\boldsymbol{\sigma}, \boldsymbol{\tau}} c_0^*(\boldsymbol{\sigma}, \boldsymbol{\tau}) c_0^*(\boldsymbol{\tau}, \boldsymbol{\sigma}) = 1, \quad (25)$$

$$\sum_{\boldsymbol{\sigma}, \boldsymbol{\tau}} c_0^*(\boldsymbol{\sigma}, \boldsymbol{\tau}) c_1^*(\boldsymbol{\tau}, \boldsymbol{\sigma}) = 0, \quad (26)$$

etc... (Note that the dependence on g and/or H is not always indicated in order to simplify the notations. We shall do the same in the following, except when needed explicitly.)

3. Mean-field limit ($z \rightarrow \infty$)

We first consider the limit $z \rightarrow \infty$ and check that the results of the mean-field model[2, 8, 12] are recovered. The calculation, which in this setting is not trivial, proceeds as follows. Inserting Eq. (21a) into Eq. (23) and performing the integrations over \mathbf{y} and \mathbf{x} , we obtain

$$c_0^*(\boldsymbol{\sigma}, \boldsymbol{\tau}) = e^{-\Lambda_0^* + gs + \sum_{\boldsymbol{\tau}'} c_1^*(\boldsymbol{\tau}', \boldsymbol{\sigma}) / \sum_{\boldsymbol{\tau}'} c_0^*(\boldsymbol{\tau}', \boldsymbol{\sigma})} \int dh \mathcal{P}(h) \prod_a \Theta(x^{*a} \sigma^a) \quad (27)$$

with

$$x^{*a}(\boldsymbol{\sigma}) = H + h + J \frac{\sum_{\boldsymbol{\tau}'} \tau'^a c_0^*(\boldsymbol{\tau}', \boldsymbol{\sigma})}{\sum_{\boldsymbol{\tau}'} c_0^*(\boldsymbol{\tau}', \boldsymbol{\sigma})}. \quad (28)$$

Since the r.h.s. of Eq. (27) does not depend on $\boldsymbol{\tau}$, c_0^* is a function of its first argument only that will be denoted as $c_0^*(\boldsymbol{\sigma})$. As a result, the quantity x^{*a} does not depend on $\boldsymbol{\sigma}$. It also does not depend on a if one assumes that all replicas are equivalent. Therefore, because of the integration over h , the only functions that differ from zero are $c_0^*(\mathbf{1})$ and $c_0^*(-\mathbf{1})$ (i.e. all σ^a are equal to 1 or -1). From Eq. (25), these two functions satisfy

$$c_0^*(\mathbf{1}) + c_0^*(-\mathbf{1}) = 1 \quad (29)$$

(the other solution of Eq. (25), $c_0^*(\mathbf{1}) + c_0^*(-\mathbf{1}) = -1$, is not physically relevant). Eq. (29) is actually a prerequisite for having a finite limit when $z \rightarrow \infty$, since it implies from Eq. (22) that $\Lambda_{-1}^* = 0$ in the expansion (17). Defining $X_1(\boldsymbol{\sigma}) = \sum_{\boldsymbol{\tau}} c_1^*(\boldsymbol{\tau}, \boldsymbol{\sigma})$ and $\Delta c_0^* = c_0^*(\mathbf{1}) - c_0^*(-\mathbf{1})$, we then rewrite Eq. (27) and (29) as

$$\frac{1}{2}[1 \pm \Delta c_0^*] = e^{-\Lambda_0^* \pm gn + X_1(\pm \mathbf{1})} \int dh \mathcal{P}(h) \Theta(\pm x^*) \quad (30)$$

and

$$e^{\Lambda_0^*} = e^{gn + X_1(\mathbf{1})} \int dh \mathcal{P}(h) \Theta(x^*) + e^{-gn + X_1(-\mathbf{1})} \int dh \mathcal{P}(h) \Theta(-x^*) \quad (31)$$

where

$$x^* = H + h + J \Delta c_0^*. \quad (32)$$

This is not yet a closed set of equations for computing Δc_0^* and Λ_0^* because the two quantities $X_1(\pm \mathbf{1})$ depend on $c_1^*(\boldsymbol{\sigma}, \boldsymbol{\tau})$. Therefore, the equations at the next order in $1/z$, Eqs. (24) and (26), must be also considered. The latter can be written as

$$(1 + \Delta c_0^*)X_1(\mathbf{1}) + (1 - \Delta c_0^*)X_1(-\mathbf{1}) = 0 \quad (33)$$

so that we only need to extract from Eq. (24) the quantity $\Delta X_1 = X_1(\mathbf{1}) - X_1(-\mathbf{1})$. A quick look at this equation shows that the solution takes the form

$$c_1^*(\boldsymbol{\sigma}, \boldsymbol{\tau}) = F(\boldsymbol{\sigma}) + e^{-\Lambda_0^* + g\boldsymbol{s} + X_1(\boldsymbol{\sigma})} I(\boldsymbol{\sigma}, \boldsymbol{\tau}) \quad (34)$$

where

$$I(\boldsymbol{\sigma}, \boldsymbol{\tau}) = -iJ \int \mathcal{P}(h) dh \int d\mathbf{x} d\mathbf{y} e^{i\mathbf{y} \cdot (\mathbf{x} - \mathbf{x}^*)} \mathbf{y} \cdot \boldsymbol{\tau} \prod_a \Theta(x^a \sigma^a) \quad (35)$$

and $F(\boldsymbol{\sigma})$ groups all other terms. The simple result follows:

$$\begin{aligned} \Delta X_1 &= \sum_{\boldsymbol{\sigma}} e^{-\Lambda_0^* + g\boldsymbol{s} + X_1(\boldsymbol{\sigma})} [I(\boldsymbol{\sigma}, \mathbf{1}) - I(\boldsymbol{\sigma}, -\mathbf{1})] \\ &= -2iJ \sum_{\boldsymbol{\sigma}} e^{-\Lambda_0^* + g\boldsymbol{s} + X_1(\boldsymbol{\sigma})} \int P(h) dh \int d\mathbf{x} \prod_a \Theta(x^a \sigma^a) \int d\mathbf{y} e^{i\mathbf{y} \cdot (\mathbf{x} - \mathbf{x}^*)} \sum_a y^a \end{aligned} \quad (36)$$

Using $-i \sum_a y^a = \partial e^{i\mathbf{y} \cdot (\mathbf{x} - \mathbf{x}^*)} / \partial x^* = \partial e^{i\mathbf{y} \cdot (\mathbf{x} - \mathbf{x}^*)} / \partial h$ and integrating by parts over h , we find that all σ^a 's must be equal in the sum over $\boldsymbol{\sigma}$, which yields

$$\Delta X_1 = 2J\mathcal{P}^* e^{-\Lambda_0^*} [e^{gn + X_1(\mathbf{1})} - e^{-gn + X_1(-\mathbf{1})}] \quad (37)$$

where \mathcal{P}^* is a shorthand for $\mathcal{P}(-H - J\Delta c_0^*)$. Eqs. (30), (31), (33), and (37) now form a closed system and Λ_0^* , Δc_0^* , and $X_1(\pm \mathbf{1})$ can be calculated in the limit $n \rightarrow 0$ by expanding in powers of n (i.e. assuming that $\Lambda_0^* = \Lambda_0^{*(0)} + n\Lambda_0^{*(1)} + \dots$, $\Delta c_0^* = \Delta c_0^{*(0)} + n\Delta c_0^{*(1)} + \dots$, and $X_1(\pm \mathbf{1}) = X_1^{(0)}(\pm \mathbf{1}) + nX_1^{(1)}(\pm \mathbf{1}) + \dots$). At the lowest order in n , this gives

$$\Lambda_0^{*(0)} = 0 \quad (38)$$

$$X_1^{(0)}(\pm \mathbf{1}) = 0 \quad (39)$$

$$\Delta c_0^{*(0)} = 2p(\Delta c_0^{*(0)}) - 1 \quad (40)$$

where $p(m) = \int_{-H-Jm}^{\infty} \mathcal{P}(h) dh = (1/2)[1 + \text{erf}([H + Jm]/\Delta\sqrt{2})]$. Note that, as stated before, $\Lambda_0^{*(0)} = 0$ is a prerequisite for a proper limit $n \rightarrow 0$. In addition, Eq. (11) readily gives

$$m_0^*(H) = \lim_{n \rightarrow 0} \sum_{\boldsymbol{\sigma}, \boldsymbol{\tau}} \sigma^a c_0^*(\boldsymbol{\sigma}, \boldsymbol{\tau}) c_0^*(\boldsymbol{\tau}, \boldsymbol{\sigma}) = \Delta c_0^{*(0)}, \quad (41)$$

so that m_0^* satisfies the self-consistent mean-field equation[2, 8, 12]

$$m_0^*(H) = \text{erf}([H + Jm_0^*(H)]/\Delta\sqrt{2}) \quad (42)$$

and does not depend of g .

At the order n , the solution of Eqs. (30),(31),(33), and (37) yields $\Lambda_0^{*(1)}(g, H) = gm_0^*(H)$ (so that $m_0^* = \partial \Lambda_0^{*(1)} / \partial g$, as it must be), and the corresponding complexity

$\Sigma_{Q,0}(g, H) = \Lambda_0^{*(1)}(g, H) - m_0^*(H)g$ is thus identically zero. In the $H - m$ plane, this means that the quenched complexity is zero when $m = m_0^*(H)$, i.e. along the mean-field loop, and is not defined otherwise. On the other hand, a trivial calculation shows that the annealed complexity[4] $\Sigma_A(m, H) = \lim_{N \rightarrow \infty} \frac{1}{N} \ln \overline{\mathcal{N}(m, H)}$ is also zero when $m = m_0^*(H)$ and strictly negative otherwise. We stress that a zero complexity does not imply that there is a unique stable state in the thermodynamic limit. The actual number of metastable states along the curve $m_0^*(H)$ can be larger than 1, even along the so-called “unstable” branch for $\Delta < \Delta_c^0$, as shown in Ref.[12].

The expressions of $\Delta c_0^{*(1)}$ and $X_1^{(1)}(\pm \mathbf{1})$, which are needed in the subsequent calculations, are given at the end of Appendix A.

4. $1/z$ correction to the quenched complexity

We now compute the $1/z$ correction to the complexity which, from Eq. (14), is given by

$$\Sigma_{Q,1}(g, H) = \Lambda_1^{*(1)}(g, H) - m_1^*(g, H)g. \quad (43)$$

To compute $\Lambda_1^{*(1)}(g, H)$ (and then $m_1^*(g, H)$ by derivation), we have to fully solve Eq. (24) so to obtain the explicit expressions of the functions $I(\boldsymbol{\sigma}, \boldsymbol{\tau})$ and $F(\boldsymbol{\sigma})$ defined by Eq. (34). After straightforward but lengthy algebraic manipulations (which are detailed in Appendix A), we find that Λ_1^* is given by

$$\begin{aligned} \Lambda_1^* = & -\frac{1}{2}[X_1(\mathbf{1})^2 c_0(\mathbf{1}) + X_1(-\mathbf{1})^2 c_0(-\mathbf{1})] - \frac{1}{2}[X_1(\mathbf{1}) + X_1(-\mathbf{1})] - \frac{1}{8}[X_1(\mathbf{1}) + X_1(-\mathbf{1})]^2 \\ & - \frac{1}{2} J \mathcal{P}^* [X_1(\mathbf{1}) - X_1(-\mathbf{1})] [e^{-\Lambda_0^* + gn + X_1(\mathbf{1})} - e^{-\Lambda_0^* - gn + X_1(-\mathbf{1})}] \\ & - \frac{1}{2} J^2 \mathcal{P}^{*2} [e^{-\Lambda_0^* + gn + X_1(\mathbf{1})} + e^{-\Lambda_0^* - gn + X_1(-\mathbf{1})}]^2 \\ & - J \mathcal{P}^* \Delta c_0^* \{ [1 + X_1(\mathbf{1})] e^{-\Lambda_0^* + gn + X_1(\mathbf{1})} - [1 + X_1(-\mathbf{1})] e^{-\Lambda_0^* - gn + X_1(-\mathbf{1})} \} \\ & + \frac{J^2}{2} (1 - \Delta c_0^{*2}) \mathcal{P}'^* [e^{-\Lambda_0^* + gn + X_1(\mathbf{1})} - e^{-\Lambda_0^* - gn + X_1(-\mathbf{1})}] + \frac{1}{2} \sum_{\boldsymbol{\sigma}} [2J \mathcal{P}^* e^{-\Lambda_0^* + gs + X_1(\boldsymbol{\sigma})}]^2 \end{aligned} \quad (44)$$

and that $X_1(\boldsymbol{\sigma})$ satisfies the equation

$$X_1(\boldsymbol{\sigma}) - X_1(\mathbf{1}) = 2J \mathcal{P}^* e^{-\Lambda_0^*} [e^{gs + X_1(\boldsymbol{\sigma})} - e^{gn + X_1(\mathbf{1})}]. \quad (45)$$

This equation plays a central role in our study and will be discussed in detail below. Let us first define the quantity $T(g, H) \equiv \sum_{\boldsymbol{\sigma}} [2J \mathcal{P}^* e^{-\Lambda_0^* + gs + X_1(\boldsymbol{\sigma})}]^2 = \sum_{\boldsymbol{\sigma}} [X_1(\boldsymbol{\sigma}) - X_1(\mathbf{1}) + 2J \mathcal{P}^* e^{-\Lambda_0^* + gn + X_1(\mathbf{1})}]^2$ and expand both sides of Eq. (44) in powers of n (with $T(g, H) = T^{(0)}(g, H) + nT^{(1)}(g, H) + \dots$). Using Eqs. (40), (41), and (A.15), this yields

$$\Lambda_1^{*(0)}(g, H) = -2J^2 \mathcal{P}_0^{*2} + \frac{1}{2} T^{(0)}(g) \quad (46)$$

and

$$\Lambda_1^{*(1)}(g, H) = g(1 - m_0^{*2}) \frac{J^2 \mathcal{P}_0'^*}{1 - 2J \mathcal{P}_0^*} (1 - 4 \frac{J \mathcal{P}_0^*}{1 - 2J \mathcal{P}_0^*}) + \frac{1}{2} T^{(1)}(g) \quad (47)$$

where \mathcal{P}_0^* is a shorthand for $\mathcal{P}(H + Jm_0^*(H))$ (i.e. $\mathcal{P}^* = \mathcal{P}_0^* + 0(n)$), and $\mathcal{P}'(h) = d\mathcal{P}(h)/dh$ (for brevity, the dependence of $T(g, H)$ on the field H is dropped). From this we obtain

$$\begin{aligned} m_1^*(g, H) &= \partial \Lambda_1^{*(1)}(g, H) / \partial g \\ &= (1 - m_0^{*2}) \frac{J^2 \mathcal{P}_0'^*}{1 - 2J\mathcal{P}_0^*} \left(1 - 4 \frac{J\mathcal{P}_0^*}{1 - 2J\mathcal{P}_0^*}\right) + \frac{1}{2} \frac{\partial T^{(1)}(g)}{\partial g} \end{aligned} \quad (48)$$

and

$$\Sigma_{Q,1}(g, H) = \frac{1}{2} \left[T^{(1)}(g) - g \frac{\partial T^{(1)}(g)}{\partial g} \right]. \quad (49)$$

(It can be checked through lengthy calculations that the same expression of $m_1^*(g, H)$ is recovered by expanding directly Eq. (11) to $O(1/z)$.)

The only remaining task is to solve Eq. (45) for $X_1(\boldsymbol{\sigma})$ and to calculate $T^{(0)}(g)$ and $T^{(1)}(g)$. This equation can be conveniently rewritten as

$$W(\boldsymbol{\sigma}) e^{W(\boldsymbol{\sigma})} = -A(g) e^{-A(g) + g(s-n)} \quad (50)$$

where $W(\boldsymbol{\sigma}) = -X_1(\boldsymbol{\sigma}) + X_1(\mathbf{1}) - A(g)$ and $A(g) = 2J\mathcal{P}^* e^{-\Lambda_0^* + gn + X_1(\mathbf{1})}$. Because of replica symmetry, $W(\boldsymbol{\sigma})$ only depends on $s = \sum_a \sigma^a$ and is a function of the single variable $\zeta(s, g) = -A(g) e^{-A(g) + g(s-n)}$. Eq. (50) becomes

$$W(\zeta) e^{W(\zeta)} = \zeta, \quad (51)$$

which tells us that $W(\zeta)$ is the so-called ‘‘Lambert function’’[16] (remarkably, this function already appears in the calculation of the average number of metastable states along the mean-field curve $m_0^*(H)$ [12]). The whole problem thus amounts to compute

$$T(g) = \sum_{\boldsymbol{\sigma}} W^2(\zeta(s, g)) \quad (52)$$

as $n \rightarrow 0$.

Let us first consider the case $g = 0$ which, as noted earlier, corresponds to the maximum of the complexity and thus yields the total number of metastable states at the field H . According to Eq. (48), in order to obtain the corresponding magnetization $m^{max}(H) = m(g = 0, H)$, one also needs to compute $\lim_{g \rightarrow 0} dT^{(1)}(g)/dg$. We then expand both sides of Eq. (51) in powers of g , using the formula for the n -th derivative of the Lambert function[16]. This allows us to perform the sum over $\boldsymbol{\sigma}$ in each term of the expansion (computing $\sum_{\boldsymbol{\sigma}} s$, $\sum_{\boldsymbol{\sigma}} s^2$, etc...). The result is then expanded in powers of n , which gives

$$T^{(0)}(g) = t^2, \quad (53)$$

and

$$T^{(1)}(g) = t^2 \ln 2 + \frac{A^{(1)}(1 - A^{(0)})}{A^{(0)}} \frac{2t^2}{1+t} g - \frac{2t^2}{1+t} g + \frac{t^2(2+t)}{(1+t)^3} g^2 + \frac{t^2(2t^2 + 9t - 8)}{6(1+t)^7} g^4 + \dots \quad (54)$$

where $A(g) = A^{(0)} + nA^{(1)}g + \dots$ and $t = W(-A^{(0)}e^{-A^{(0)}})$. Since $\Lambda_0^{*(0)} = X_1^{(0)}(\mathbf{1}) = 0$ (Eqs. (38) and (39)), one has

$$A^{(0)} = 2J\mathcal{P}_0^*, \quad (55)$$

and, using Eqs. (A.15),

$$A^{(1)} = (1 - m_0^*) \frac{2J\mathcal{P}_0^*}{1 - 2J\mathcal{P}_0^*} + 2(1 - m_0^{*2}) \frac{J^2\mathcal{P}_0^{*'}}{[1 - 2J\mathcal{P}_0^*]^2}. \quad (56)$$

A question now needs to be addressed: which branch of $W(\zeta)$ should be chosen? Recall that the Lambert function has two real branches, $W_0(\zeta)$ and $W_{-1}(\zeta)$, with a branch point at $\zeta = -1/e$ [16]. The principal branch $W_0(\zeta)$ takes on values between -1 to $+\infty$ for $\zeta \geq -1/e$ (with $W_0(0) = 0$) and $W_{-1}(\zeta)$ takes on values between $-\infty$ and -1 for $-1/e \leq \zeta \leq 0$. Accordingly one has

$$\begin{aligned} W_0(-xe^{-x}) &= -x \quad \text{if } x \leq 1 \\ W_0(-xe^{-x}) &= -x' \quad \text{if } x \geq 1 \end{aligned} \quad (57)$$

where x' is the solution (smaller than 1) of the equation $x'e^{-x'} = xe^{-x}$. Similarly,

$$\begin{aligned} W_{-1}(-xe^{-x}) &= -x \quad \text{if } x \geq 1 \\ W_{-1}(-xe^{-x}) &= -x' \quad \text{if } x \leq 1 \end{aligned} \quad (58)$$

where $x' \geq 1$.

The choice of the branch is determined by the fact that $\Lambda^{*(0)}$ must vanish at all orders in $1/z$ in order to get a proper limit when $n \rightarrow 0$. Eq. (46) then implies that

$$T^{(0)}(g) = 4J^2\mathcal{P}_0^{*2} = A^{(0)2} \quad (59)$$

whence $t = W(-A^{(0)}e^{-A^{(0)}}) = -A^{(0)}$ in Eq. (53). Therefore, according to Eqs. (57) and (58), one has to choose the principal branch $W_0(\zeta)$ for $A^{(0)} < 1$ and the branch $W_{-1}(\zeta)$ for $A^{(0)} > 1$ (note that W_0 is the only branch that comes into play in the calculations of Ref. [12]). The series (54) then becomes

$$\begin{aligned} T^{(1)}(g) &= A^{(0)2} \ln 2 + 2A^{(0)}A^{(1)}g - \frac{2A^{(0)2}}{1 - A^{(0)}}g + \frac{A^{(0)2}(2 - A^{(0)})}{(1 - A^{(0)})^3}g^2 \\ &+ \frac{A^{(0)2}(2A^{(0)2} - 9A^{(0)} - 8)}{6(1 - A^{(0)})^7}g^4 \dots \end{aligned} \quad (60)$$

so that, from Eqs. (48) and (49),

$$m_1^{max}(H) = -m_0^* \frac{4J^2\mathcal{P}_0^{*2}}{1 - 2J\mathcal{P}_0^*} + (1 - m_0^{*2}) \frac{J^2\mathcal{P}_0^{*'}}{1 - 2J\mathcal{P}_0^*}, \quad (61)$$

and

$$\Sigma_{Q,1}^{max}(H) \equiv \Sigma_{Q,1}(g = 0, H) = 2J^2\mathcal{P}_0^{*2} \ln 2. \quad (62)$$

This result will be commented on in the next section. More generally, the problem is that the series (60) is strongly divergent when g is large. We therefore need to find an integral representation that allows the sum to make sense for an arbitrary value of g . With this in mind, we write $\zeta(s, g) = -A(g)e^{-A(g)}[1 + (e^{g(s-n)} - 1)]$ and formally

expand $W^2(\zeta(s, g))$ around $-A(g)e^{-A(g)}$ in Eq. (52), which again allows us to perform the sum over σ . Expanding the result in powers of n , we get

$$T^{(1)}(g) = A^{(0)2} \ln 2 + g \left[\frac{A^{(1)}(1 - A^{(0)})}{A^{(0)}} - 1 \right] \zeta_0^{(0)} \frac{dW^2}{d\zeta} \Big|_{\zeta=\zeta_0^{(0)}} + \sum_{p=1}^{\infty} \frac{\zeta_0^{(0)p}}{p!} \frac{d^p W^2}{d\zeta^p} \Big|_{\zeta=\zeta_0^{(0)}} \sum_{q=1}^p (-1)^{p+q} \binom{p}{q} \ln \cosh(qg) \quad (63)$$

where $\zeta_0^{(0)} = A^{(0)}e^{-A^{(0)}}$. The first few terms explicitly read

$$T^{(1)}(g) = A^{(0)2} \ln 2 + 2A^{(0)}A^{(1)}g + \frac{2A^{(0)2}}{1 - A^{(0)}} [\ln \cosh(g) - g] + \frac{A^{(0)2}(A^{(0)2} - A^{(0)} - 1)}{(1 - A^{(0)})^3} [2 \ln \cosh(g) - \ln \cosh(2g)] + \frac{1}{3} \frac{A^{(0)3}(2A^{(0)3} - 5A^{(0)2} + 6)}{(1 - A^{(0)})^5} [3 \ln \cosh(g) - 3 \ln \cosh(2g) + \ln \cosh(3g)] \dots \quad (64)$$

This of course gives back the power series (60) when expanding in powers of g . To find an integral representation of (63), we then use the identity[17]

$$\tanh(qg) = \frac{2\pi}{g} \int_0^{\infty} dx \frac{\sin(2q\pi x)}{\sinh(\pi^2 x/g)} \quad (65)$$

which yields by integration

$$\ln \cosh(qg) = \int_0^{\infty} dx \frac{1 - \cos(2q\pi x)}{x \sinh(\pi^2 x/g)} \quad (66)$$

(the study is now restricted to $g > 0$ but we know that in the end $\Sigma_Q(g, H)$ and $m^*(g, H)$ are even and odd functions of g , respectively). As will be explained just below, it is convenient to split the domain of integration in Eq. (66) into the successive intervals $[0, 1]$, $[1, 2]$, $[2, 3]$, etc..., and to change x to $1 - x$ in the interval $[1/2, 1]$. This yields

$$\ln \cosh(qg) = \int_0^{1/2} dx f(x, g) [1 - \cos(2q\pi x)] \quad (67)$$

where

$$f(x, g) = \sum_{k=-\infty}^{\infty} \frac{1}{(x+k) \sinh(\pi^2(x+k)/g)}. \quad (68)$$

Using $\sum_{q=1}^p (-1)^q \binom{p}{q} = -1$, we then have

$$\sum_{q=1}^p (-1)^q \binom{p}{q} \ln \cosh(qg) = - \int_0^{1/2} dx f(x, g) \Re(1 - e^{-2i\pi x})^p, \quad (69)$$

where \Re denotes the real part, so that the series (63) admits the following integral representation

$$T^{(1)}(g) = A^{(0)2} \ln 2 + 2A^{(0)}A^{(1)}g - \frac{2A^{(0)2}}{1 - A^{(0)}}g + \int_0^{1/2} dx f(x, g) [A^{(0)2} - \Re\{W^2(-A^{(0)}e^{-A^{(0)}}e^{-2i\pi x})\}], \quad (70)$$

where we have interchanged summation and integration. (A priori this is not justified since the series $\sum_{p=1}^{\infty} (-1)^p \frac{\zeta_0^{(0)p}}{p!} \frac{d^p W^2}{d\zeta^p} \Big|_{\zeta=\zeta_0^{(0)}} (1 - e^{-2i\pi x})^p$ is not uniformly convergent for x in $[0, 1/2]$; on the other hand, we have checked numerically that the power series (60) is asymptotic to the result of Eq. (70) for sufficiently small g , even for $A^{(0)} > 1$.) Note that it is essential that the path in the complex plane does not cross the branch cuts of W_0 and W_{-1} when integrating over x in Eq. (70). The branch cut of W_0 is $\{\zeta : -\infty < \zeta \leq -1/e\}$ whereas W_{-1} has the double branch-cut $\{\zeta : -\infty < \zeta \leq -1/e\}$ and $\{\zeta : -\infty < \zeta \leq 0\}$ [16]. Since $-A^{(0)}e^{-A^{(0)}} \geq -1/e$, the restriction of the domain of integration to the interval $[0, 1/2]$ ensures that the imaginary part $\Im\{-A^{(0)}e^{-A^{(0)}}e^{-2i\pi x}\} \geq 0$, which explains that we use the integral representation (67) instead of (65).

Replacing $T^{(1)}(g)$ in Eq. (48) and (49) by its expression (70), and using Eqs. (55) and (56), we finally obtain

$$m_1^*(g, H) = -m_0^* \frac{4J^2 \mathcal{P}_0^{*2}}{1 - 2J\mathcal{P}_0^*} + (1 - m_0^{*2}) \frac{J^2 \mathcal{P}_0^{*'}}{1 - 2J\mathcal{P}_0^*} + \frac{1}{2} \frac{\partial C(g, H)}{\partial g} \quad (71)$$

and

$$\Sigma_{Q,1}(g, H) = 2J^2 \mathcal{P}_0^{*2} \ln 2 + \frac{1}{2} \left(C(g, H) - g \frac{\partial C(g, H)}{\partial g} \right) \quad (72)$$

where

$$\begin{aligned} C(g, H) &\equiv T^{(1)}(g) - A^{(0)2} \ln 2 - 2A^{(0)} A^{(1)} g + \frac{2A^{(0)2}}{1 - A^{(0)}} g \\ &= \int_0^{1/2} dx f(x, g) [A^{(0)2} - \Re\{W^2(-A^{(0)}e^{-A^{(0)}}e^{-2i\pi x})\}]. \end{aligned} \quad (73)$$

Especially important are the limits $g \rightarrow \pm\infty$, as discussed in Ref.[12]. It turns out that further analytical progress can be made in this case. Indeed, one can show that $f(x, g) \sim g/\sin^2(\pi x) - 2\ln(2)$ when $g \rightarrow +\infty$. As a result, it is found that

$$\begin{aligned} m_1^*(g \rightarrow +\infty, H) &= -m_0^* \frac{4J^2 \mathcal{P}_0^{*2}}{1 - 2J\mathcal{P}_0^*} + (1 - m_0^{*2}) \frac{J^2 \mathcal{P}_0^{*'}}{1 - 2J\mathcal{P}_0^*} \\ &\quad + \frac{1}{2} \int_0^{1/2} dx \frac{A^{(0)2} - \Re\{W^2(-A^{(0)}e^{-A^{(0)}}e^{-2i\pi x})\}}{\sin^2(\pi x)}, \end{aligned} \quad (74)$$

and, after some additional manipulations,

$$\Sigma_{Q,1}(g \rightarrow +\infty, H) = \ln 2 \int_0^{1/2} dx \Re\{W^2(-A^{(0)}e^{-A^{(0)}}e^{-2i\pi x})\} = -\frac{\ln 2}{2\pi} \Im\left\{\frac{w^3}{3} + \frac{w^2}{2}\right\} \quad (75)$$

where $w = W(+A^{(0)}e^{-A^{(0)}})$.

With these expressions, we can now study the behavior of the quenched complexity in the field-magnetization plane and compare with the hysteresis loop. (In Appendix C, we indicate a change of variable in Eqs. (73) and (74) which is better suited for numerical calculations.)

5. Results and discussion

The exact equations that describes the saturation hysteresis loop on a Bethe lattice were obtained in Ref.[9] and the expansion of these equations to $O(1/z)$ is worked out in Appendix B. Let us recall again that the main feature is the existence of an out-of-equilibrium phase transition for $z \geq 4$ in the thermodynamic limit. Whereas the hysteresis loop is smooth for $\Delta > \Delta_c(z)$, it has a jump for $\Delta < \Delta_c(z)$ that results from the flip of a finite fraction of spins (a macroscopic “avalanche”). The critical disorder $\Delta_c(z)$ increases with z (see e.g. Fig. 1 in Ref.[18]) and the mean-field behavior described by Eq.(42) is recovered when $z \rightarrow \infty$ [18]. From a mathematical point of view the transition for $\Delta < \Delta_c(z)$ is due to a saddle-node bifurcation[9]: the self-consistent equation (B.2) (that corresponds to an increasing applied field) has three real roots in the range $H_1(\Delta) < H < H_2(\Delta)$ and two of the solutions coalesce and become complex at the branching fields H_1 and H_2 (see Fig. 3 below). As H increases, the quantity $U(H)$ defined by Eq. (B.2) follows initially the lowest solution and then jumps to the highest one at $H = H_2(\Delta)$. The symmetric behavior is observed when decreasing the field. Whether or not the third “unstable” root and the corresponding reentrant branches of the hysteresis loop have a physical meaning will be discussed below. Note that an intermediate branch is already present in the mean-field equation (42) below the critical disorder $\Delta_c^0 = J\sqrt{2/\pi}$ [8]. Since $dm_0^*/dH < 0$, this branch is also generally described as “unstable”, which is actually a misleading terminology since some metastable states may be present, as shown in Ref.[12]. The important point for the following discussion is that the key quantity $A^{(0)} = 2J\mathcal{P}(H + Jm_0^*(H))$ is smaller than 1 for $\Delta > \Delta_c^0$ and on the stable portions of the mean-field curve for $\Delta < \Delta_c^0$. On the other hand, it is larger than 1 along the intermediate “unstable” branch ($A^{(0)} = 1$ at the spinodal endpoints).

5.1. $\Delta > \Delta_c^0$

We first consider the strong-disorder regime in which the loop is smooth in the thermodynamic limit. For simplicity, we assume that $\Delta > \Delta_c^0 > \Delta_c(z)$ so that the mean-field magnetization curve is also smooth. Then $A^{(0)} < 1$ and $W = W_0$ in the equations of the preceding section. To illustrate numerically the general behavior, we take $\Delta = 1$ and $z = 30$.

In Fig. 1, we first show the hysteresis loop computed from the equations of Ref. [9] (see also Eqs. (B.1) and (B.2)) and the mean-field magnetization curve $m_0(H)$. We also plot the loop resulting from the expansion in $1/z$, $m(H) = m_0(H) + (1/z)m_1(H)$ where $m_1(H)$ is given by Eqs. (B.19) and (B.20). As can be seen, the exact result is accurately described by the first two terms in the $1/z$ expansion for the chosen value $z = 30$.

The curves $m^*(g, H) = m_0^*(H) + (1/z)m_1^*(g, H)$ versus g and $\Sigma_Q(m, H) = (1/z)\Sigma_{Q,1}(m, H)$ versus m following the results of the preceding section are plotted in Figs. 2 (a) and 2 (b), respectively, for $H = 0$. The results are qualitatively similar for any other value of the field. As g varies from $-\infty$ to $+\infty$, the magnetization $m^*(g, H)$

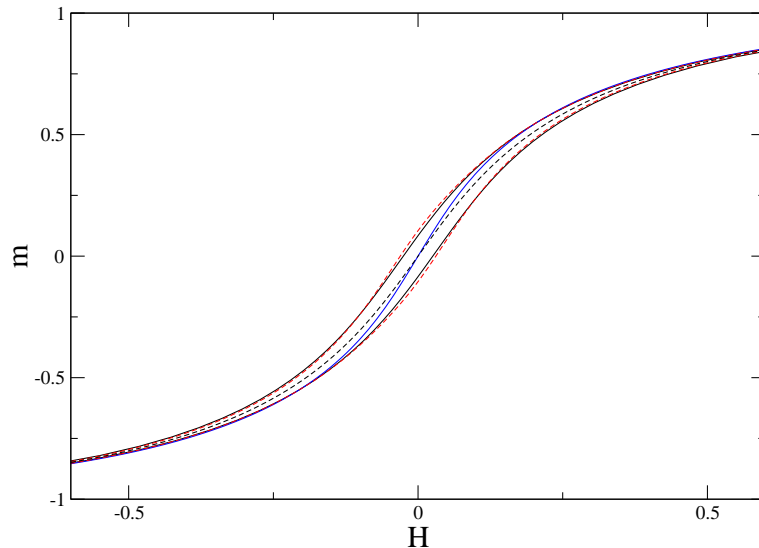


Figure 1. Hysteresis loop for $\Delta = 1$ and $z = 30$ (solid black line). At the scale of the figure, the $1/z$ expansion at first order (red dashed line) reproduces accurately the exact result. The solid blue line is the mean-field magnetization curve and the dashed black line is the locus of the maximum of the complexity.

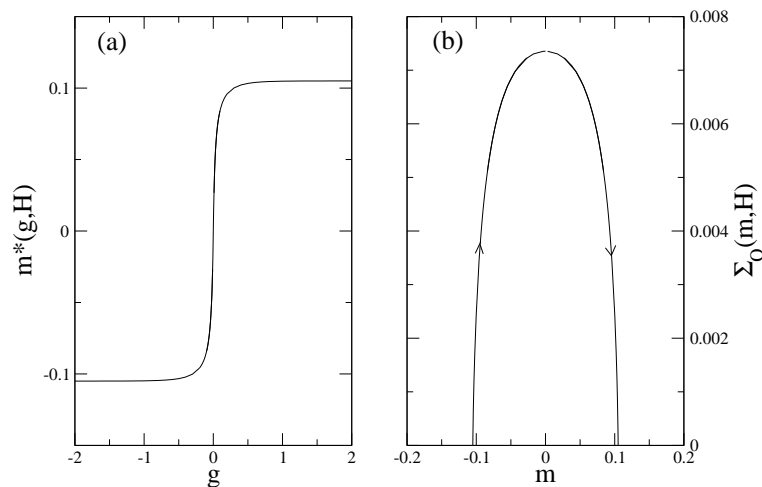


Figure 2. Magnetization $m^*(g, H) = m_0^*(H) + (1/z)m_1^*(g, H)$ (left panel) and quenched complexity $\Sigma_Q(m, H) = (1/z)\Sigma_{Q,1}(m, H)$ (right panel) for $\Delta = 1$, $z = 30$, and $H = 0$. The arrows in (b) indicate that g increases from $-\infty$ and $+\infty$ along the curve. $\Sigma_Q(g, H) \rightarrow 0$ when $g \rightarrow \pm\infty$ so that $\Sigma_Q(m, H) = 0$ on the hysteresis loop (see text).

increases monotonously, and the complexity, as a function of m , has a shape similar to that observed for $z = 2$ [4]. In particular, the slope is infinite when $g \rightarrow \pm\infty$, as a consequence of the Legendre relation $g = -\partial\Sigma_Q(m, H)/\partial m$.

By studying the behavior as $g \rightarrow \pm\infty$, we can now answer the question that motivated the present study: is the saturation hysteresis loop the boundary of the

region in the $H - m$ plane where the quenched complexity is strictly positive? In the strong-disorder regime, the answer to this question is positive (at least at the order $1/z$). Indeed, when $W = W_0$, the integral in the r.h.s. of Eq. (74) is equal to $2A^{(0)2}/(1 - A^{(0)}) = 8J^2\mathcal{P}_0^{*2}/(1 - 2J\mathcal{P}_0^*)$. As a result, Eq. (74) identifies with Eq. (B.20) which describes the descending branch of the hysteresis loop. (Similarly, the ascending branch is recovered as $g \rightarrow -\infty$.) Moreover, when $w = W_0(+A^{(0)}e^{-A^{(0)}})$, one has $\Im\{\frac{w^3}{3} + \frac{w^2}{2}\} = 0$ in Eq. (75) so that $\Sigma_{Q,1}(g \rightarrow +\infty, H)$, the $1/z$ correction to the complexity along the hysteresis loop, is also zero. These two results prove that the curve $\Sigma_Q(m, H) = 0$ coincides with the saturation hysteresis loop at this order[7]. (These results can also be obtained directly from Eq. (63) by expanding formally in powers of $A^{(0)}$, and taking the limit $g \rightarrow +\infty$: one finds that $T^{(1)}(g) \sim 2A^{(0)}A^{(1)}g + O(e^{-4g})$, which yields $C(g, H) \sim 2A^{(0)2}/(1 - A^{(0)})g - A^{(0)2} \ln 2 + O(e^{-4g})$.)

5.2. $\Delta < \Delta_c(z)$

We now turn to the low-disorder regime, illustrated by the case $\Delta = 0.3$ and $z = 100$. The hysteresis loop obtained from the equations of Ref.[9] is shown in Fig. 3 (for clarity, the mean-field magnetization curve $m_0(H)$ is only shown in Fig. 4 that zooms in the lower part of Fig. 3).

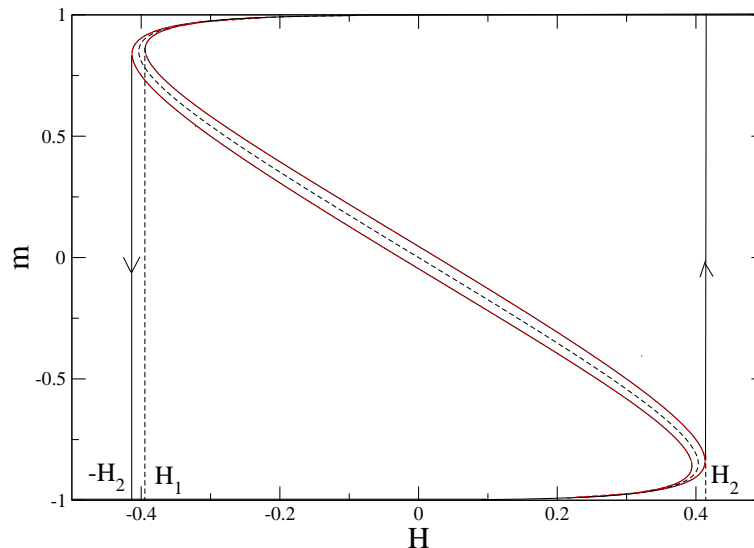


Figure 3. Hysteresis loop for $\Delta = 0.3$ and $z = 100$ (solid black line) showing jumps at the fields H_2 and $-H_2$. The two intermediate branches corresponding to the “unstable” root of the self-consistent equation of Ref. [9] are included. The red dashed lines represent the “renormalized” curves $H(m) = H_0(m) + (1/z)H_1(m)$ and the dashed black line is the locus of the maxima of the complexity. H_1 and H_2 are the branching fields associated with Eq. (B.2) (see text).

The hysteresis loop has now a jump that occurs at $H = H_2$ (resp. $-H_2$) when increasing (resp. decreasing) the applied field. For completeness we also plot in the figure the reentrant branches that correspond to the “unstable” root of the self-consistent

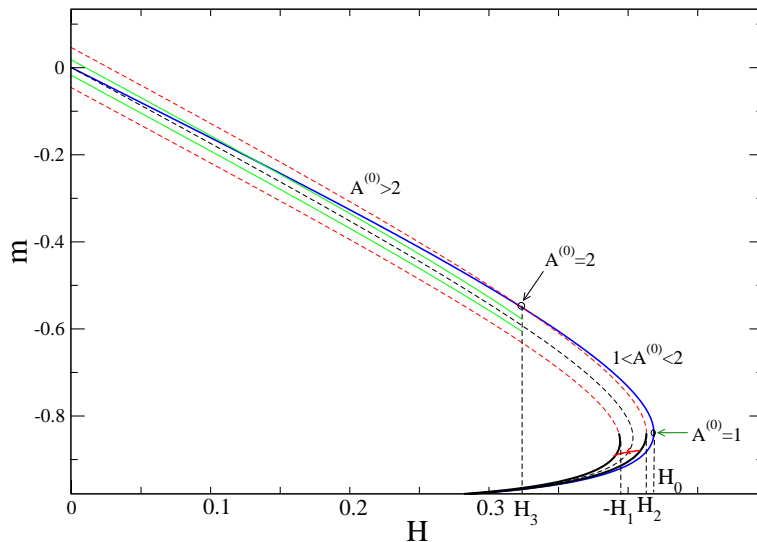


Figure 4. Zoom on the lower part of Fig. 3. The blue curve is the mean-field magnetization and the arrows indicate the points on this curve that correspond to $A^{(0)} = 1$ ($H = H_0$) and $A^{(0)} = 2$ ($H = H_3$). The complexity vanishes along the two “stable” branches in the lower part of the loop (bold solid lines) but remains finite along the two green curves in the central part of the loop for $0 \leq H \leq H_3$. There is an exponential number of metastable states in the strip between the two green curves and this strip is narrower than the region delimited by the dashed red lines. A first-order reversal curve is also shown in the lower part of the loop (solid red line).

equation of Ref. [9]: for $H_1 < H < H_2$ or $-H_2 < H < -H_1$ when increasing or decreasing the field, respectively. The red dashed lines represent the “renormalized” curves $H(m) = H_0(m) + H_1(m)/z + \dots$, where $H_0(m)$ is the inverse function of $m_0(H)$ (i.e. $H_0(m_0(H)) = H$) and $H_1(m)$ is given by Eq. (B.21). As explained at the end of Appendix B, this “renormalization” of the $1/z$ expansion is necessary because the expansion $m(H) = m_0(H) + m_1(H)/z + \dots$ diverges when H approaches the mean-field branching fields, that is when $A^{(0)} \rightarrow 1$. This problem can be circumvented by working at constant magnetization instead of constant field and expanding H instead of m . At the scale of Fig. 3, the resulting curves are indistinguishable from the exact ones, including the reentrant parts. We also display in the figure the locus of the maxima of the complexity which will be commented on later.

We now discuss the results for the magnetization $m^*(g, H)$ and the quenched complexity $\Sigma_Q(m, H) = (1/z)\Sigma_{Q,1}(m, H)$. For clarity, we only focus on the lower part of the loop (i.e. for $m < 0$) as the upper one can be obtained via the symmetry $m(-H) = -m(H)$. A priori, three values of the external field are noteworthy, as indicated in Fig. 4: the two branching fields $-H_1 \approx 0.391$ and $H_2 \approx 0.413$, and the mean-field branching field $H_0 \approx 0.418$ (note that H_2 is close to, but smaller than, H_0). As will be seen below, the field $H_3 \approx 0.323$ such that $A^{(0)}(H_3) = 2$, with $m_0^*(H_3)$ being the “unstable” solution of Eq. (42), will also play a role.

We first consider the lower part of the loop for an applied field $H < -H_1$. \mathcal{P}_0^* is

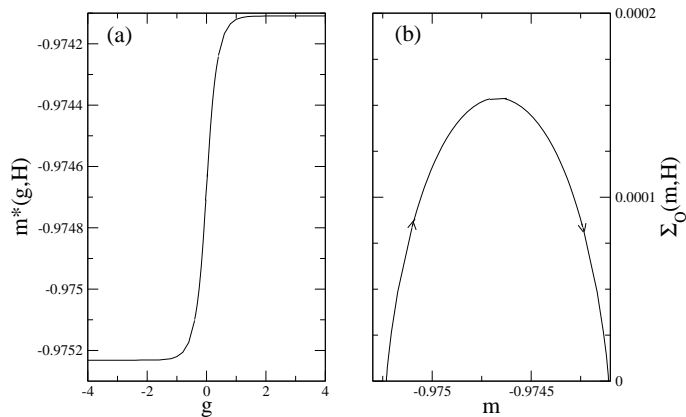


Figure 5. Same as Fig. 2 for $\Delta = 0.3$, $z = 100$, and $H = 0.3$ (lower part of the hysteresis loop).

then computed with the solution of Eq. (42) that corresponds to the lowest value of the magnetization m_0^* . Then $dm_0^*/dH > 0$ and $A^{(0)} < 1$ so that $W = W_0$ in the equations of the preceding section. As a result, the qualitative behavior of $m^*(g, H)$ and $\Sigma_Q(m, H)$ is the same as in the strong-disorder regime: the region between the two branches of the hysteresis contains an exponential number of metastable states and the quenched complexity vanishes exactly along the two branches. This is illustrated in Fig. 5 (a) and 5 (b) for $H = 0.3$ ($m_0^* \approx -0.975$ and $A^{(0)} \approx 0.210$). It must be emphasized that this part of the descending branch of the hysteresis (reached in the limit $g \rightarrow +\infty$) is physically accessible via a first-order reversal curve starting from the ascending branch, i.e. a protocol where H is first increased to a value less than H_2 and then decreased. Such a curve is shown in Fig. 4 (red line). States that can be reached in this way are called H -states[19] and it thus appears that there is an exponentially large number of metastable states when H -states are present (most of the metastable states however are not H -states).

The behavior is different in the central part of the loop, and we need to distinguish the two cases $H < H_3$ and $H_3 < H$. The first one is illustrated in Figs. 6 (a) and 6 (b) for $H = 0$. \mathcal{P}_0^* is then calculated with $m_0^* = 0$ so that $A^{(0)} \approx 2.660 > 1$ and one has to take $W = W_{-1}$ in Eqs. (71)-(75). As can be seen in Fig. 6 (b), the main difference with the case $A^{(0)} < 1$ is that the complexity does not vanish when $g \rightarrow \pm\infty$. (When setting $w = W_{-1}(+A^{(0)}e^{-A^{(0)}})$ in Eq. (75), $\Im\{\frac{w^3}{3} + \frac{w^2}{2}\}$ is no more equal to zero.) Moreover, the integral in the r.h.s. of Eq. (74) is not equal to $2A^{(0)2}/(1 - A^{(0)})$ so that Eq. (74) does not identify with Eq. (B.20). As shown in Fig. 4, the actual region where the number of metastable states is exponentially large, bounded by the two curves $m^*(H) = m_0^*(H) + (1/z)m_1^*(g \rightarrow \pm\infty, H)$ shown in green in the figure, is narrower than the region delimited by the reentrant branches of the hysteresis loop (red dashed lines in Fig. 4). This feature is in agreement with the numerical estimations of Ref.[6] for $z = 4$. Therefore, these reentrant branches, which correspond to the “unstable” root of the self-consistent equation of Ref.[9], bear no relation to the quenched complexity and

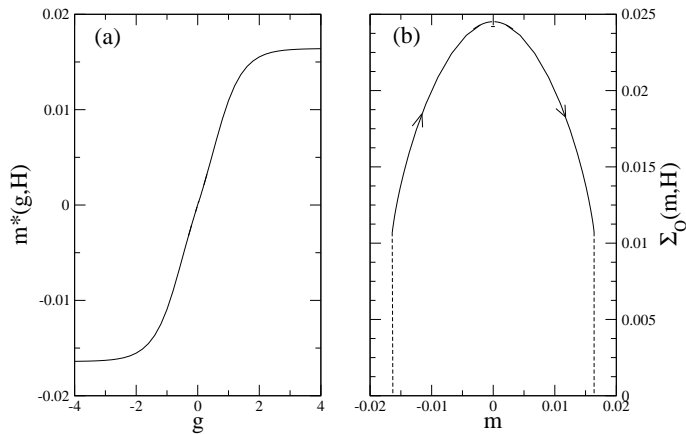


Figure 6. Same as Fig. 2 for $\Delta = 0.3$, $z = 100$, and $H = 0$ (central part of the hysteresis loop). Note that the complexity tends to a non-zero value (≈ 0.0107) when $g \rightarrow \pm\infty$. There are no metastable states with $|m| \gtrsim 0.016$.

do not seem to have a physical meaning.

As H increases from 0 and $m_0^*(H)$ decreases along the reentrant part of the mean-field curve, $A^{(0)}$ decreases and the minimum value of the complexity $\Sigma_Q(g \rightarrow \pm\infty, H)$ also decreases. Eventually, this quantity becomes negative for $A^{(0)} \approx 1.9885$, which corresponds to a field that is slightly larger than H_3 . In fact, as soon as $H > H_3$, a new feature appears, which is illustrated in Figs. 7 (a) and 7 (b) for $H = 0.36$ ($m_0^* = -0.627$ and $A^{(0)} \approx 1.787$): the magnetization $m^*(g, H)$ is no more a monotonously increasing function of g ; in other words, the mapping $\{m^*(g, H), \Sigma_Q(g, H)\} \mapsto \Sigma_Q(m, H)$ is not unique. This induces the awkward behavior of $\Sigma_Q(m, H)$ observed in Fig. 7 (b). Moreover, there is a whole range of m where $\Sigma_Q(m, H)$ is negative.

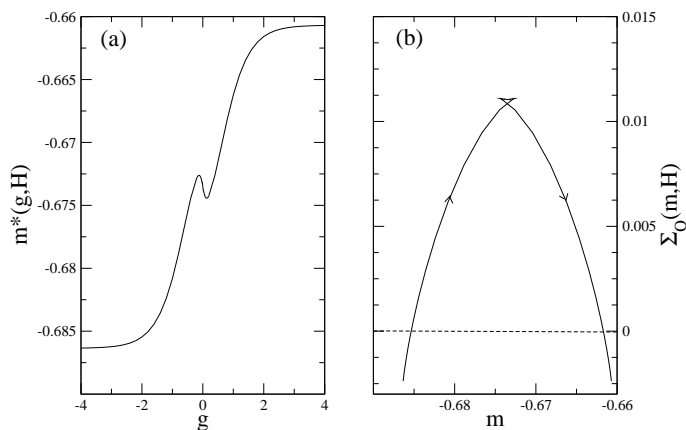


Figure 7. Same as Fig. 2 for $\Delta = 0.3$, $z = 100$, and $H = 0.36$ (central part of the hysteresis loop).

The fact that $dm_1^*(g, H)/dg|_{g=0} = (1/2) d^2C(g, H)/dg^2|_{g=0}$ is negative for $1 < A^{(0)} < 2$ is already clear from Eq. (60), the power series of $T^{(1)}(g)$ (for $H = H_3$,

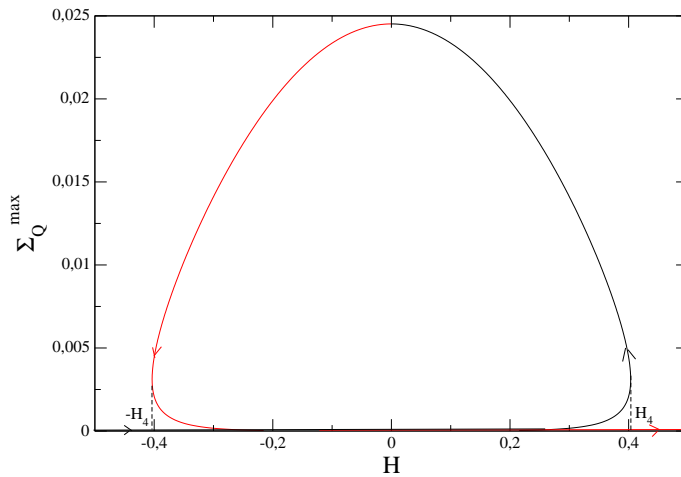


Figure 8. Total complexity $\Sigma_Q^{max}(H) = (1/z)\Sigma_{Q,1}^{max}(H)$ for $\Delta = 0.3$ and $z = 100$ (see note [21]). As one follows the loop, the complexity increases from 0 to ≈ 0.0245 (black curve) and then decreases again to 0 (red curve), as indicated by the arrows.

$m^*(g, H)$ has an inflexion point at $g = 0$). Unfortunately, this signals that the solution of the saddle-point equations is unstable or inconsistent and that there is a flaw in the analytical calculations of the preceding section. Indeed, $\Sigma_Q(m, H)$ must be always smaller than $\Sigma_Q^{max}(H) = \Sigma_Q(g = 0, H)$, which implies that $\partial^2 \Sigma_Q(g, H) / \partial g^2 |_{m=cst.} = \partial^2 \Lambda^{*(1)}(g, H) / \partial g^2 = \partial m^*(g, H) / \partial g$ must be positive at $g = 0$ [20]. It must be also emphasized that the quenched complexity is a quantity that cannot become negative. Despite our effort, we have not succeeded in finding the origin of the problem. We have considered various possibilities, including a breaking of symmetry of the replica vector \mathbf{g} or the existence of complex saddles, but unsuccessfully [21]. Therefore, for $H_3 < H < -H_1$, we do not know the actual behavior of the complexity in the central region of the loop, and for $-H_1 < H < H_2$, we can only predict that the complexity vanishes on the lower branch of the loop (since this branch is obtained with $A^{(0)} < 1$ and $W = W_0$). The analytical behavior of the complexity in this intermediate region is obviously rather complicated.

On the other hand, the value of the *total* quenched complexity $\Sigma_Q^{max}(H) = \Sigma_Q(g = 0, H)$ is known in the whole $H - m$ plane (cf. Eq. (62)), as well as the corresponding magnetization $m^{max}(H)$. These two quantities, properly “renormalized” in order to avoid a spurious divergence when $A^{(0)} \rightarrow 1$ [22], are shown in Fig. 8 ($\Sigma_Q^{max}(H)$) and Figs. 3 and 4 ($m^{max}(H)$). Σ_Q^{max} is multivalued for $-H_4 < H < H_4$ where $H_4 = (H_2 - H_1)/2$ and it is maximum in the central part of the hysteresis loop. Therefore, the typical magnetization of the metastable states is actually a discontinuous function of H with a negative slope around $H = 0$. The surprising result that the magnetization of the most probable metastable states goes oppositely with the applied field is in full agreement with the numerical results of Ref.[6] (see Figs. 16 and 17 in this reference).

Let us stress again that all the above results concern the behavior of the *quenched*

complexity, associated with the typical number of metastable states. The annealed complexity is much more easily computed (along the lines of Ref.[4]) but much less informative. It indeed remains positive outside the saturation hysteresis loop for finite z , as shown in Ref.[4], which signals the presence of “atypical” metastable states in this region. The two complexities only coincide along the mean-field magnetization curve in the limit $z \rightarrow \infty$ and are then equal to zero.

6. Conclusion

The main result of this paper concerns the organization of the metastable states of the RFIM in the field-magnetization plane and its relation with the saturation hysteresis loop. Calculations have been performed on a Bethe lattice of connectivity z in the large- z limit to order $1/z$. Although some pieces of the solution are still missing, the following conclusions can be made, that complete and confirm earlier computations:

1) When the hysteresis loop is smooth in the thermodynamic limit (strong-disorder regime), the quenched complexity $\Sigma_Q(m, H)$ is strictly positive everywhere inside the loop, i.e. the number of the metastable states with a given magnetization increases exponentially with the system size, and it vanishes exactly along the loop. This is also the behavior computed analytically in one dimension[4] and observed numerically for $z = 4$ and on the cubic lattice[6]. It is therefore quite reasonable to conclude that this is a general result. It would be nice, of course, to have another, more direct derivation of this property.

2) When the hysteresis loop is discontinuous (low-disorder regime), the quenched complexity is positive in two sectors:

First, in the two regions (before and after the jump in magnetization) that can be reached by a field history starting from one of the saturated states. It appears that there is an exponentially large number of metastable states when H -states (i.e. field-reachable states[19]) are present, even if most of these metastable states are not H -states. The complexity vanishes along the two branches of the loop that coincide with the envelope of the H -states. In these two regions, the typical magnetization of the metastable states (i.e. the magnetization of the states whose number dominates the whole distribution) increases with H .

Second, in a strip of finite width (of order $1/z$ in our calculations) around the mean-field magnetization curve. This region in the middle of the loop is inaccessible to any field history starting from the saturated states. In addition, the complexity does not go continuously to zero on the borders of the strip, which moreover do not identify with the “unstable” branches computed from the fixed-point equations of Ref.[9]. It is in this strip that the number of metastable states is the largest and the typical magnetization decreases with H .

The above results are in agreement with the numerical study of Ref.[6] for $z = 4$ and for the cubic lattice and they suggest that in the low-disorder regime the region of positive (quenched) complexity evolves with connectivity as depicted in Fig. 9. We

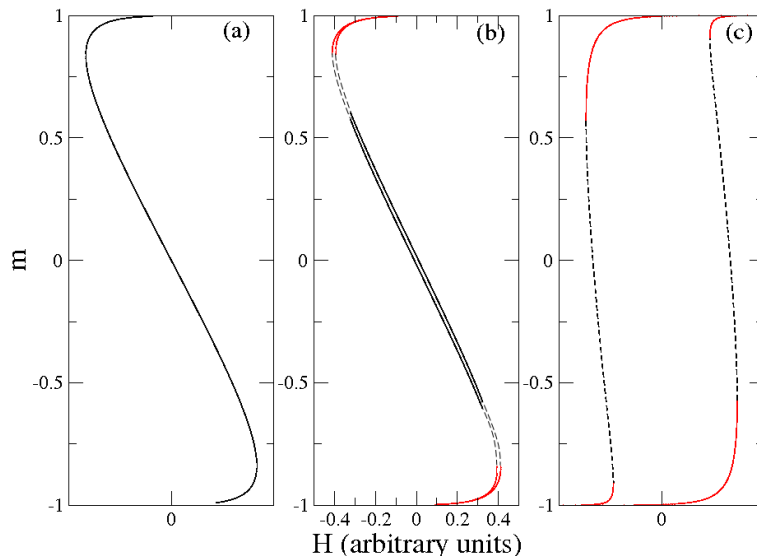


Figure 9. Evolution of the envelope of the typical metastable states in the field-magnetization plane in the low-disorder regime as a function of the connectivity z : (a) mean-field limit ($z = \infty$), (b) order $1/z$, (c) $z = 4$. The complexity vanishes along the parts of the curves drawn in red. Certain parts are still putative (dashed lines).

recall that a few metastable states are already present along the intermediate part of the mean-field curve[12]. Although the precise behavior of the complexity in the vicinity of the “knees” is still unknown (and is certainly different on the Bethe and on euclidian lattices), it is now clear that the discontinuity in the hysteresis loop associated with a macroscopic avalanche is due to the existence of a gap in the magnetization of the metastable states for a range of applied field. Consequently, by controlling the magnetization instead of the magnetic field[11], one should observe a reentrant loop, as indeed observed in some magnetic materials[1] and other disordered systems[23, 24]. Finally, one may wonder whether the most numerous, hence probable, states in the middle of the loop are accessible dynamically; it is, however, dubious that this can be achieved by performing a deep quench from $T = \infty$ to $T = 0$ at a fixed field[25].

To conclude, we have related the out-of-equilibrium disorder-induced transition in the RFIM at zero temperature to the distribution of the metastable states in the field-magnetization plane (thus replacing the dynamic problem by a purely static calculation). An interesting challenge would be to describe in a similar way other out-of-equilibrium field-driven transitions, for instance the depinning transition[26, 27]. In this case, one must take explicitly into account the geometry of the lattice.

Acknowledgments

MLR thanks T. Munakata for many fruitful discussions during his visit to Kyoto University.

Appendix A. Calculation of the complexity at the order $1/z$

In this appendix, we detail the calculation of the complexity at the order $1/z$, solving Eq. (24).

We first note a difficulty in the $1/z$ expansion of the function $c^*(\boldsymbol{\sigma}, \boldsymbol{\tau})$ arising from the presence of terms like $\mathbf{y} \cdot \boldsymbol{\tau}$ in Eq. (24), $(\mathbf{y} \cdot \boldsymbol{\tau})^2$ at the next order, etc... These terms come from the expansion of $e^{-i\frac{J}{z}\mathbf{y} \cdot \boldsymbol{\tau}}$ and they introduce successive derivatives of the Dirac δ -function when integrating over y^a . This makes the integrals ill-defined (or even divergent) and therefore this hierarchy of equations for $c_1^*(\boldsymbol{\sigma}, \boldsymbol{\tau})$, $c_2^*(\boldsymbol{\sigma}, \boldsymbol{\tau})$, etc... may just be considered as a formal and convenient way of book-keeping all the contributions at a certain order in $1/z$. To circumvent the difficulty, however, one can simply re-exponentiate the problematic terms. Consider for instance the quantity $I(\boldsymbol{\sigma}, \boldsymbol{\tau})$ defined by Eqs. (34) and (35). It can be rewritten as

$$\begin{aligned} I(\boldsymbol{\sigma}, \boldsymbol{\tau}) &= \int dh \mathcal{P}(h) \int d\mathbf{x} d\mathbf{y} e^{i\mathbf{y} \cdot (\mathbf{x} - \mathbf{x}^*)} \prod_a \Theta(x^a \sigma^a) \lim_{z \rightarrow \infty} z [e^{-i\frac{J}{z}\mathbf{y} \cdot \boldsymbol{\tau}} - 1] \\ &= \lim_{z \rightarrow \infty} z \int dh \mathcal{P}(h) \left\{ \prod_a \Theta(\sigma^a [x^* + \frac{J}{z}\tau^a]) - \prod_a \Theta(\sigma^a x^*) \right\}, \quad (\text{A.1}) \end{aligned}$$

which readily yields

$$\begin{aligned} I(\pm \mathbf{1}, \boldsymbol{\tau}) &= J\mathcal{P}^* [(1 \pm \tau) \prod_a \delta_K(\tau^a; \tau) - 1] \\ I(\boldsymbol{\sigma}, \boldsymbol{\tau}) &= 2J\mathcal{P}^* \prod_a \delta_K(\sigma^a; \tau^a) \quad \text{if } \boldsymbol{\sigma} \neq \pm \mathbf{1}. \quad (\text{A.2}) \end{aligned}$$

where δ_K is the Kronecker symbol. This shows that the dependence of $c_1^*(\boldsymbol{\sigma}, \boldsymbol{\tau})$ on $\boldsymbol{\sigma}$ and $\boldsymbol{\tau}$ is rather simple.

We now consider the quantity $X_1(\boldsymbol{\sigma}) = \sum_{\boldsymbol{\tau}} c_1^*(\boldsymbol{\tau}, \boldsymbol{\sigma})$. From Eq. (34), it satisfies the self-consistent equation

$$X_1(\boldsymbol{\sigma}) = \sum_{\boldsymbol{\tau}} F(\boldsymbol{\tau}) + e^{-\Lambda_0^*} \sum_{\boldsymbol{\tau}} e^{gt + X_1(\boldsymbol{\tau})} I(\boldsymbol{\tau}, \boldsymbol{\sigma}) \quad (\text{A.3})$$

where $t = \sum_a \tau^a$. Using Eq. (A.2), we find after some algebra

$$\begin{aligned} X_1(\pm \mathbf{1}) &= \sum_{\boldsymbol{\tau}} F(\boldsymbol{\tau}) \pm J\mathcal{P}^* e^{-\Lambda_0^*} [e^{gn + X_1(\mathbf{1})} - e^{-gn + X_1(-\mathbf{1})}] \\ X_1(\boldsymbol{\sigma}) &= \sum_{\boldsymbol{\tau}} F(\boldsymbol{\tau}) + J\mathcal{P}^* e^{-\Lambda_0^*} [2e^{gs + X_1(\boldsymbol{\sigma})} - e^{gn + X_1(\mathbf{1})} - e^{-gn + X_1(-\mathbf{1})}] \quad \text{if } \boldsymbol{\sigma} \neq \pm \mathbf{1} \end{aligned} \quad (\text{A.4})$$

so that

$$\sum_{\boldsymbol{\tau}} F(\boldsymbol{\tau}) = \frac{1}{2} [X_1(\mathbf{1}) + X_1(-\mathbf{1})] \quad (\text{A.5})$$

and

$$X_1(\boldsymbol{\sigma}) = X_1(\mathbf{1}) + 2J\mathcal{P}^* e^{-\Lambda_0^*} [e^{gs + X_1(\boldsymbol{\sigma})} - e^{gn + X_1(\mathbf{1})}]. \quad (\text{A.6})$$

This is the crucial self-consistency equation (45), valid for all $\boldsymbol{\sigma}$.

We then calculate the quantity $F(\boldsymbol{\sigma})$ defined by Eq.(34). After some manipulations, we obtain from Eqs. (21b), (24) and (34)

$$\begin{aligned}
 F(\boldsymbol{\sigma}) &= [-\Lambda_1^* - X_1(\boldsymbol{\sigma}) + X_2(\boldsymbol{\sigma}) - \frac{1}{2}X_1(\boldsymbol{\sigma})^2]c_0^*(\boldsymbol{\sigma}) \prod_a \delta_K(\sigma^a; \boldsymbol{\sigma}) \\
 &+ e^{-\Lambda_0^* + gs + X_1(\boldsymbol{\sigma})} \sum_{\boldsymbol{\tau}} I(\boldsymbol{\sigma}, \boldsymbol{\tau}) c_1^*(\boldsymbol{\tau}, \boldsymbol{\sigma}) \\
 &+ e^{-\Lambda_0^* + gs + X_1(\boldsymbol{\sigma})} \int \mathcal{P}(h) dh \int d\mathbf{x} d\mathbf{y} e^{i\mathbf{y} \cdot (\mathbf{x} - \mathbf{x}^*)} \prod_a \Theta(x^a \sigma^a) \left\{ iJ\Delta c_0^* [1 + X_1(\boldsymbol{\sigma})] \right. \\
 &\times \left. \sum_a y^a - \frac{J^2}{2}(1 - \Delta c_0^{*2}) \left(\sum_a y^a \right)^2 \right\} \quad (\text{A.7})
 \end{aligned}$$

where $X_2(\boldsymbol{\sigma}) = \sum_{\boldsymbol{\tau}} c_2^*(\boldsymbol{\tau}, \boldsymbol{\sigma})$. The last term is computed by integration by parts over h , which gives

$$\begin{aligned}
 F(\boldsymbol{\sigma}) &= [-\Lambda_1^* - X_1(\boldsymbol{\sigma}) + X_2(\boldsymbol{\sigma}) - \frac{1}{2}X_1(\boldsymbol{\sigma})^2]c_0^*(\boldsymbol{\sigma}) \prod_a \delta_K(\sigma^a; \boldsymbol{\sigma}) \\
 &+ e^{-\Lambda_0^* + gs + X_1(\boldsymbol{\sigma})} \sum_{\boldsymbol{\tau}} I(\boldsymbol{\sigma}, \boldsymbol{\tau}) c_1^*(\boldsymbol{\tau}, \boldsymbol{\sigma}) \\
 &+ \sigma e^{-\Lambda_0^* + gs + X_1(\boldsymbol{\sigma})} \left\{ -J\Delta c_0^* [1 + X_1(\boldsymbol{\sigma})] \mathcal{P}^* + \frac{J^2}{2}(1 - \Delta c_0^{*2}) \mathcal{P}'^* \right\} \prod_a \delta_K(\sigma^a; \boldsymbol{\sigma}) \quad (\text{A.8})
 \end{aligned}$$

where $\mathcal{P}'(h)$ is the derivative of $\mathcal{P}(h)$ with respect to h . It thus remains to calculate $\sum_{\boldsymbol{\tau}} I(\boldsymbol{\sigma}, \boldsymbol{\tau}) c_1^*(\boldsymbol{\tau}, \boldsymbol{\sigma})$ and $X_2(\pm \mathbf{1}) = \sum_{\boldsymbol{\tau}} c_2^*(\boldsymbol{\tau}, \pm \mathbf{1})$. Using Eqs. (34) and (A.2), we find after some algebra

$$\begin{aligned}
 \sum_{\boldsymbol{\tau}} I(\pm \mathbf{1}, \boldsymbol{\tau}) c_1^*(\boldsymbol{\tau}, \pm \mathbf{1}) &= J\mathcal{P}^* [2F(\pm \mathbf{1}) - X_1(\pm \mathbf{1}) + 2J\mathcal{P}^* e^{-\Lambda_0^* \pm gn + X_1(\pm \mathbf{1})}] \\
 \sum_{\boldsymbol{\tau}} I(\boldsymbol{\sigma}, \boldsymbol{\tau}) c_1^*(\boldsymbol{\tau}, \boldsymbol{\sigma}) &= 2J\mathcal{P}^* F(\boldsymbol{\sigma}) + 4J^2 \mathcal{P}^{*2} e^{-\Lambda_0^* + gs + X_1(\boldsymbol{\sigma})} \\
 &= 2J\mathcal{P}^* [F(\boldsymbol{\sigma}) - W(\boldsymbol{\sigma})] \quad \text{if } \boldsymbol{\sigma} \neq \pm \mathbf{1} \quad (\text{A.9})
 \end{aligned}$$

where $W(\boldsymbol{\sigma}) = -X_1(\boldsymbol{\sigma}) + X_1(\mathbf{1}) - A(g)$ and $A(g) = 2J\mathcal{P}^* e^{-\Lambda_0^* + gn + X_1(\mathbf{1})}$. Inserting into Eq. (A.7), we obtain

$$\begin{aligned}
 [1 - 2J\mathcal{P}^* e^{-\Lambda_0^* \pm gn + X_1(\pm \mathbf{1})}] F(\pm \mathbf{1}) &= [-\Lambda_1^* - X_1(\pm \mathbf{1}) + X_2(\pm \mathbf{1}) - \frac{1}{2}X_1(\pm \mathbf{1})^2] c_0^*(\pm \mathbf{1}) \\
 &- J\mathcal{P}^* e^{-\Lambda_0^* \pm gn + X_1(\pm \mathbf{1})} [X_1(\pm \mathbf{1}) - 2J\mathcal{P}^* e^{-\Lambda_0^* \pm gn + X_1(\pm \mathbf{1})}] \\
 &\pm e^{-\Lambda_0^* \pm gn + X_1(\pm \mathbf{1})} \left\{ -J\Delta c_0^* [1 + X_1(\pm \mathbf{1})] \mathcal{P}^* + \frac{J^2}{2}(1 - \Delta c_0^{*2}) \mathcal{P}'^* \right\} \quad (\text{A.10})
 \end{aligned}$$

and

$$[1 - 2J\mathcal{P}^* e^{-\Lambda_0^* + gs + X_1(\boldsymbol{\sigma})}] F(\boldsymbol{\sigma}) = [2J\mathcal{P}^* e^{-\Lambda_0^* + gs + X_1(\boldsymbol{\sigma})}]^2 = W^2(\boldsymbol{\sigma}) \quad \text{if } \boldsymbol{\sigma} \neq \pm \mathbf{1} \quad (\text{A.11})$$

where we have used Eq. (A.6) and the definition of $W(\boldsymbol{\sigma})$.

In order to compute $X_2(\pm \mathbf{1})$, we consider the normalization equation (10) at the order $1/z^2$, which reads

$$2 \sum_{\boldsymbol{\sigma}, \boldsymbol{\tau}} c_0^*(\boldsymbol{\sigma}, \boldsymbol{\tau}) c_2^*(\boldsymbol{\tau}, \boldsymbol{\sigma}) + \sum_{\boldsymbol{\sigma}, \boldsymbol{\tau}} c_1^*(\boldsymbol{\sigma}, \boldsymbol{\tau}) c_1^*(\boldsymbol{\tau}, \boldsymbol{\sigma}) = 0, \quad (\text{A.12})$$

whence

$$c_0(\mathbf{1})X_2(\mathbf{1}) + c_0(-\mathbf{1})X_2(-\mathbf{1}) = -\frac{1}{2} \sum_{\boldsymbol{\sigma}, \boldsymbol{\tau}} c_1^*(\boldsymbol{\sigma}, \boldsymbol{\tau}) c_1^*(\boldsymbol{\tau}, \boldsymbol{\sigma}). \quad (\text{A.13})$$

Using Eqs. (34), (A.5) and (A.11), we find

$$\begin{aligned} c_0(\mathbf{1})X_2(\mathbf{1}) + c_0(-\mathbf{1})X_2(-\mathbf{1}) &= F(\mathbf{1})[1 - 2J\mathcal{P}^* e^{-\Lambda_0^* + gn + X_1(\mathbf{1})}] + F(-\mathbf{1})[1 - 2J\mathcal{P}^* e^{-\Lambda_0^* - gn + X_1(-\mathbf{1})}] \\ &\quad - \frac{1}{8}[X_1(\mathbf{1}) + X_1(-\mathbf{1})]^2 - \frac{1}{2}[X_1(\mathbf{1}) + X_1(-\mathbf{1})][1 - J\mathcal{P}^* e^{-\Lambda_0^*}(e^{gn + X_1(\mathbf{1})} + e^{-gn + X_1(-\mathbf{1})})] \\ &\quad - J^2\mathcal{P}^{*2} \left[\frac{5}{2} e^{2[-\Lambda_0^* + gn + X_1(\mathbf{1})]} + \frac{5}{2} e^{2[-\Lambda_0^* - gn + X_1(-\mathbf{1})]} + e^{-2\Lambda_0^* + X_1(\mathbf{1}) + X_1(-\mathbf{1})} \right] \\ &\quad + \frac{1}{2}T(g) \end{aligned} \quad (\text{A.14})$$

where we have introduced $T(g) = \sum_{\boldsymbol{\sigma}} W^2(\boldsymbol{\sigma})$ (cf. Eq. (52)).

Inserting this into Eqs.(A.10), adding the two equations for $F(\mathbf{1})$ and $F(-\mathbf{1})$, and using the normalization equation (26), we finally obtain Eq. (44). (Note that, remarkably, the terms involving $F(\pm \mathbf{1})$ have cancelled out so that there is no need to compute $X_2(\mathbf{1})$ and $X_2(-\mathbf{1})$ separately, which would imply to also consider the equation for $c_2(\boldsymbol{\sigma}, \boldsymbol{\tau})$.)

In order to calculate $\Lambda_1^{*(1)}$, one also needs the following expressions of $\Delta c_0^{*(1)}$ and $X_1^{(1)}(\pm \mathbf{1})$, solutions of Eqs. (30), (31), (33), and (37) at the order n ,

$$\begin{aligned} \Delta c_0^{*(1)} &= g \frac{1 - m_0^{*2}}{[1 - 2J\mathcal{P}_0^*]^2} \\ X_1^{(1)}(\pm \mathbf{1}) &= \pm g(1 \pm m_0^*) \frac{2J\mathcal{P}_0^*}{1 - 2J\mathcal{P}_0^*}. \end{aligned} \quad (\text{A.15})$$

Appendix B. Calculation of the hysteresis loop at the order $1/z$

In this Appendix, we compute the hysteresis loop at the order $1/z$, starting from the equations derived by Dhar et al.[9]. The approach to the mean-field behavior has been studied numerically in Ref.[18], but, as far as we know, the explicit calculation has only been performed in the limit $z \rightarrow \infty$. According to Ref.[9], the magnetization $m(H)$ along the ascending branch of the hysteresis loop is given by

$$\frac{1}{2}[m(H) + 1] = \sum_{k=0}^z \binom{z}{k} U^k (1 - U)^{z-k} p_k \quad (\text{B.1})$$

where $U(H)$ is solution of the self-consistent equation

$$U = \sum_{k=0}^{z-1} \binom{z-1}{k} U^k (1 - U)^{z-1-k} p_k \quad (\text{B.2})$$

and $p_k(H) = \int_{-H+J(1-\frac{2k}{z})}^{+\infty} \mathcal{P}(h)dh$ is the probability for a spin down to flip up at the field H when k of its nearest neighbours are up[9] (J has been rescaled by z). In order to compute the $O(1/z)$ correction, we assume the expansion $U = U_0 + U_1/z + U_2/z^2 + \dots$, and, anticipating the fact that the sums in Eqs. (B.1) and (B.2) are dominated by the term corresponding to $k = zU_0$, we change to the variable $t = k/z$ and replace the sums by integrals that can be computed asymptotically by the Laplace method[28]. Eq. (B.1) then becomes

$$\frac{1}{2}(m(H) + 1) \simeq z \int_0^1 dt \exp[\ln \binom{z}{zt} + zt \ln U + z(1-t) \ln(1-U)]p(t) \quad (\text{B.3})$$

with $p(t) = \int_{-H+J(1-2t)}^{\infty} \mathcal{P}(h)dh$. Similarly, Eq. (B.2), which is conveniently rewritten as $U(1-U) = \sum_{k=0}^z \frac{z-k}{z} \binom{z}{k} U^k (1-U)^{z-k} p_k$, becomes

$$U(1-U) \simeq z \int_0^1 dt (1-t) \exp[\ln \binom{z}{zt} + zt \ln U + z(1-t) \ln(1-U)]p(t) . \quad (\text{B.4})$$

Expanding U and $m(H)$, and using the Stirling approximation for the binomial coefficient in the large- z limit, we find

$$\frac{1}{2}(m_0(H) + 1) + \frac{1}{2z}m_1(H) + \dots \simeq \sqrt{\frac{z}{2\pi}} \int_0^1 dt e^{z\phi(t)} f(t) [1 + \frac{1}{z}g(t) + \dots] \quad (\text{B.5})$$

and

$$U_0(1-U_0) + \frac{1}{z}U_1(1-2U_0) + \dots \simeq \sqrt{\frac{z}{2\pi}} \int_0^1 dt e^{z\phi(t)} (1-t)f(t) [1 + \frac{1}{z}g(t) + \dots] \quad (\text{B.6})$$

where

$$\phi(t) = t \ln \frac{U_0}{t} + (1-t) \ln \frac{1-U_0}{1-t} \quad (\text{B.7})$$

$$f(t) = \frac{p(t)}{\sqrt{t(1-t)}} \exp\left[t \frac{U_1}{U_0} - (1-t) \frac{U_1}{1-U_0}\right] \quad (\text{B.8})$$

$$g(t) = t \left[\frac{U_2}{U_0} - \frac{U_1^2}{2U_0^2} \right] - (1-t) \left[\frac{U_2}{1-U_0} + \frac{U_1^2}{2(1-U_0)^2} \right] + \frac{1}{12} \left[1 - \frac{1}{t(1-t)} \right] . \quad (\text{B.9})$$

The function $\phi(t)$ is maximum for $t = U_0$, with $\phi(U_0) = 0$, $[-\phi''(U_0)]^{-1/2} = \sqrt{U_0(1-U_0)}$ and $f(U_0) = p(U_0)/\sqrt{U_0(1-U_0)}$, so that, at the leading order, one obtains from Eq. (B.5)

$$\frac{1}{2}(m_0(H) + 1) = p(U_0) \quad (\text{B.10})$$

and, from Eq. (B.6),

$$U_0 = p(U_0) \quad (\text{B.11})$$

Using the definition of $p(t)$, this readily yields Eq. (42), the self-consistent mean-field equation. To compute the terms of order $1/z$ we need to take into account the first

correction to the asymptotic behavior in the Laplace method [28]. This gives from Eq. (B.5)

$$\frac{1}{2}m_1(H) = \sqrt{U_0(1-U_0)} \left\{ f(U_0)g(U_0) - \frac{f''(U_0)}{2\phi''(U_0)} + \frac{f(U_0)\phi''''(U_0)}{8[\phi''(U_0)]^2} + \frac{f'(U_0)\phi'''(U_0)}{2[\phi''(U_0)]^2} - \frac{5f(U_0)[\phi'''(U_0)]^2}{24[\phi''(U_0)]^3} \right\} \quad (\text{B.12})$$

and, from Eq. (B.6), a similar expression for $U_1(1-2U_0)$ with $f(t)$ replaced by $(1-t)f(t)$. Using $U_0 = (m_0 + 1)/2$, we have

$$-\frac{1}{2\phi''(U_0)} = \frac{1-m_0^2}{8} \quad (\text{B.13})$$

$$\frac{\phi''''(U_0)}{8[\phi''(U_0)]^2} = -\frac{1+3m_0^2}{4(1-m_0^2)} \quad (\text{B.14})$$

$$\frac{\phi'''(U_0)}{2[\phi''(U_0)]^2} = -\frac{m_0}{2} \quad (\text{B.15})$$

$$-\frac{5[\phi'''(U_0)]^2}{24[\phi''(U_0)]^3} = \frac{5m_0^2}{6(1-m_0^2)}. \quad (\text{B.16})$$

After some algebra, we obtain

$$m_1 = 4J\mathcal{P}_0^*U_1 + (1-m_0^2)J^2\mathcal{P}_0^{*\prime} \quad (\text{B.17})$$

and

$$U_1 = -(1+m_0)\frac{J\mathcal{P}_0^*}{1-2J\mathcal{P}_0^*} + \frac{1-m_0^2}{2}J\mathcal{P}_0^{*\prime}, \quad (\text{B.18})$$

where $2J\mathcal{P}_0^* \equiv 2J\mathcal{P}(H+Jm_0) = p'(c)$ and $\mathcal{P}_0^{*\prime} = P'(H+Jm_0)$, using the notations of sections III and IV (with m_0^* replaced by m_0). Hence finally,

$$m_1(H) = -(1+m_0)\frac{4J^2\mathcal{P}_0^{*2}}{1-2J\mathcal{P}_0^*} + (1-m_0^2)\frac{J^2\mathcal{P}_0^{*\prime}}{1-2J\mathcal{P}_0^*}. \quad (\text{B.19})$$

Similarly, along the descending branch (using the symmetry $H \rightarrow -H$, $m \rightarrow -m$),

$$m_1(H) = (1-m_0)\frac{4J^2\mathcal{P}_0^{*2}}{1-2J\mathcal{P}_0^*} + (1-m_0^2)\frac{J^2\mathcal{P}_0^{*\prime}}{1-2J\mathcal{P}_0^*}. \quad (\text{B.20})$$

For $\Delta < \Delta_c^0 = J\sqrt{2/\pi}$, the function $m_0(H)$ is multivalued and Eqs. (B.19) and (B.20) diverge at the mean-field spinodal where $\partial m_0/\partial H = 2\mathcal{P}_0^*/(1-2J\mathcal{P}_0^*) \rightarrow \infty$. This problem may be cured by considering the field as a function of the magnetization and expanding H as $H(m) = H_0(m) + H_1(m)/z + H_2(m)/z^2 + \dots$, where $H_0(m)$ is the inverse function of $m_0(H)$, the solution of Eq. (42). Then $H_1(m) = -m_1(H_0(m))/[\partial m_0/\partial H|_{H=H_0(m)}] = -m_1(H_0(m))[1-2J\mathcal{P}_0^*(H_0(m))]/2\mathcal{P}_0^*(H_0(m))$ and from Eq. (B.19) we obtain

$$H_1(m) = 2(1+m)J^2\mathcal{P}_0^*(m) - \frac{1}{2}(1-m^2)\frac{J^2\mathcal{P}_0^{*\prime}(m)}{\mathcal{P}_0^*(m)} \quad (\text{B.21})$$

along the ascending branch.

Appendix C. Alternative expression of $C(g, H)$

Eqs. (73) and (74) are not convenient for numerical calculation because the Lambert function must be evaluated in the complex plane. This problem can be circumvented by changing the integration variable. From the equation $W(\zeta)e^{W(\zeta)} = \zeta$, we have

$$\begin{aligned} A^{(0)} e^{-A^{(0)}} \cos 2\pi x &= -e^u [u \cos v - v \sin v] \\ A^{(0)} e^{-A^{(0)}} \sin 2\pi x &= e^u [v \cos v + u \sin v] \end{aligned} \quad (\text{C.1})$$

where $u(x)$ and $v(x)$ are respectively the real and imaginary parts of $W(-A^{(0)} e^{-A^{(0)}} e^{-2i\pi x})$. For $W = W_0$ (resp. $W = W_{-1}$), u is a continuous function of x that monotonically increases (resp. decreases) as x increases from 0 to 1 and v can be univoquely expressed as a function of u through the relation

$$v(u) = \pm (A^{(0)2} e^{-2(A^{(0)}+u)} - u^2)^{1/2} \quad (\text{C.2})$$

where the signs $+$ and $-$ refer to $W = W_0$ and $W = W_{-1}$, respectively. A careful analysis shows that the inverse function $x(u)$ is given by

$$\begin{aligned} x(u) &= \frac{1}{2\pi} \arctan \frac{u \tan v + v}{v \tan v - u}, \quad -A^{(0)} \leq u \leq u_1 \text{ (resp. } u_1 < u \leq -A^{(0)}) \\ x(u) &= \frac{1}{2} + \frac{1}{2\pi} \arctan \frac{u \tan v + v}{v \tan v - u}, \quad u_1 < u \leq u_0 \text{ (resp. } u_0 \leq u \leq u_1) \end{aligned} \quad (\text{C.3})$$

where $u_0 = u(x = 1/2) = \Re\{W(A^{(0)} e^{-A^{(0)}})\}$ and $u_1 = u(x = 1/4) = \Re\{W(iA^{(0)} e^{-A^{(0)}})\}$. Making the change of variable $x \rightarrow u$ in Eq. (73), we then obtain

$$C(g, H) = \frac{1}{2\pi} \int_{-A^{(0)}}^{u_0} du [f(x(u), g) + f(1 - x(u), g)] \frac{[A^{(0)2} - u^2 + v^2][(1 + u)^2 + v^2]}{v}, \quad (\text{C.4})$$

where the proper expression of $x(u)$ must be used in each interval $[-A^{(0)}, u_1]$ and $]u_1, u_0]$ (resp. $]u_0, u_1]$ and $]u_1, -A^{(0)}]$). Similarly, in Eq. (74), by using $\frac{1}{\sin^2(\pi x)} dx = -\frac{d}{\pi dx} \cot(\pi x) dx = -\frac{d}{\pi du} \cot(\pi x(u)) du$ and integrating by parts, we get

$$\frac{C(g, H)}{g} \rightarrow -\frac{2}{\pi} \int_{-A^{(0)}}^{u_0} du \frac{2u + u^2 + v^2}{\tan(\pi x(u))} \quad (\text{C.5})$$

when $g \rightarrow +\infty$. Note that the integrand in Eq. (C.4) diverges for both $u \rightarrow -A^{(0)}$ and $u \rightarrow u_0$ when $W = W_0$ (in both cases $v \rightarrow 0$), whereas it only diverges for $u \rightarrow -A^{(0)}$ when $W = W_{-1}$. However, these are inverse square-root singularities and the integral is finite, as it must be.

4. References

- [1] Bertotti G, 1998 *Hysteresis in Magnetism*, Academic Press
- [2] Sethna J P, Dahmen K A, Kartha S, Krumhansl J A, Roberts B W and Shore J D, 1993 *Phys. Rev. Lett.* **70**, 3347
- [3] Pierce M S *et al*, 2007 *Phys. Rev. B* **75**, 144406

- [4] Detcherry F, Rosinberg M L and Tarjus G, 2005 *Eur. Phys. J. B* **44**, 327
- [5] Sethna J P, Dahmen K A and Perković O, 2006 in *The Science of Hysteresis*, edited by Bertotti G and Mayergoyz I, Academic Press, Amsterdam
- [6] Pérez-Reche F J, Rosinberg M L and Tarjus G, 2008 *Phys. Rev. B* **77**, 064422
- [7] Note that in each disorder realization, at a given external field H , there is a unique metastable state associated with the hysteresis loop, as a result of the no-passing rule[2]. On the loop, the complexity is therefore always equal to zero. The nontrivial issue is to know whether there is, or not, a finite region inside the loop that also has a zero complexity. The results show that this is not true when the loop is continuous.
- [8] Dahmen K and Sethna J P, 1996 *Phys. Rev. B* **53**, 14872
- [9] Dhar D, Shukla P and Sethna J P, 1997 *J. Phys. A: Math. Gen.* **30**, 5259
- [10] For a strongly asymmetric distribution of the random field, a jump in the magnetization occurs on the square lattice, see Sabhapandit S., Dhar D. and Shukla P., 2002 *Phys. Rev. Lett.* **88**, 197202. However, for a symmetric Gaussian distribution, simulations are inconclusive.
- [11] Illa X, Rosinberg M L and Vives E, 2006 *Phys. Rev. B* **74**, 224403
- [12] Rosinberg M L, Tarjus G and Pérez-Reche F J, 2008, *J. Stat. Mech.* P10004
- [13] Monasson R, 1998 *J. Phys. A: Math. Gen.* **31**, 513
- [14] Berg J and Sellito M, 2002 *Phys. Rev. E* **65**, 016115
- [15] Eqs. (5-7) summarize Eqs.(11-17) of Ref. [4]. Note that the functions $c(\tau, \sigma)$ defined in Ref. [4] above Eq. (9) have been rescaled by the factor $\sqrt{z/\gamma}$ in order to eliminate an artificial dependence on γ . The definition of Λ has also been slightly changed, so that the present equations are a bit different and simpler than those of Ref. [4]. (Note also that the term $-\frac{z}{2} \sum_{\sigma, \tau} c(\sigma, \tau)c(\tau, \sigma)$ in Eq. (6) is missing in Eq. (23) of Ref. [4].)
- [16] Corless R M, Gonnet G H, Hare D E G, Jeffrey D J and Knuth D E, 1996 *Adv. Comput. Math.***5**, 329 (1996); Corless R M, Jeffrey D J, and D. E. Knuth D E, 1997 in *Proceedings of the International Symposium on Symbolic and Algebraic Computation*
- [17] Prudnikov A P, Brychkov Yu A and Marichev O I, 2002 *Integrals and Series*, vol. 1, Taylor and Francis
- [18] Illa X, Shukla P and Vives E, 2006 *Phys. Rev. B* **73**, 092414
- [19] Basso V and Magni A, 2004 *Physica B* **343**, 275
- [20] This seems to imply that $\Sigma_Q(g, H)$ reaches a minimum at $g = 0$ and not a maximum. However, one must recall that the contour of integration for g^a lies originally on the imaginary axis (this comes from the integral representation of a delta function[4]). Therefore the Hessian must be taken with respect to ig^a , which transforms the original maximum into a minimum.
- [21] In all the calculations of section IV, it is assumed that the solution $g^*(m, H)$ of the saddle-point equation (11) in the limit $n \rightarrow 0$ is real. Since the original contour lies on the imaginary axis, it is then understood that it is deformed to pass by the real saddle-point. In other words, if one considers Eq. (71) as an equation for g for a given value of m_1^* , the solution is supposed to be real. However, for some values of m_1^* , one can also find complex (and conjugate) values of g such that the imaginary part of $\partial C(g, H)/\partial g$ is zero and the real part satisfies Eq. (71) (Eq. (65) can be indeed extended to the complex plane[17]). However, in the range of magnetizations where the real solution is obviously wrong (i.e. the region around $g = 0$ in Fig. 7(a) where $dm^*(g, H)/dg$ is negative), there are no complex solutions. Note finally that a replica-symmetry breaking of the spin-glass type due the constraint of fixed magnetization has not been considered here. This, however, may occur as suggested by the calculation of the ground-state via the cavity method (T. Castellani, F. Krzakala, F. Ricci-Tersenghi, and L. Zdeborova, private communication).
- [22] $m_1^{max}(H)$ as given by Eq. (61) diverges when $A^{(0)} = 2J\mathcal{P}_0^* \rightarrow 1$. Therefore, one must “renormalize” the $1/z$ expansion as explained at the end of Appendix B and consider the field $H^{max}(m) = H_0(m) - (1/z)m_1^{max}(H_0(m))[1 - 2J\mathcal{P}_0^*(H_0(m))]/2\mathcal{P}_0^*(H_0(m))$. The complexity Σ_Q^{max} , which only depends on $A^{(0)}$, is then considered as a function of H^{max} .
- [23] Bonnot E, Romero R, Illa X, Mañosa L, Planes A and Vives E, 2007 *Phys. Rev. B* **76**, 064105

- [24] Kierlik E, Puibasset J and Tarjus G, 2008 *Preprint* cond-mat/0809.2314
- [25] Rosinberg M L (unpublished results)
- [26] See e.g. Koiler B and Robbins M O, 2000 *Phys. Rev. B* **62**, 5771
- [27] Pérez-Reche F J, Truskinovsky L and Zanzotto G, 2008 *Preprint* cond-mat/0807.3011
- [28] Bender C M and Orszag S A , 1987 *Advanced Mathematical Methods for Scientists and Engineers*, McGraw-Hill, 3rd edition, p. 272